

# Topological active matter

Suraj Shankar,<sup>1</sup> Anton Souslov,<sup>2</sup> Mark J. Bowick,<sup>3</sup> M. Cristina Marchetti,<sup>4</sup> and Vincenzo Vitelli<sup>5, 6, 7</sup>

<sup>1</sup>*Department of Physics, Harvard University, Cambridge, MA 02318, USA*

<sup>2</sup>*Department of Physics, University of Bath, Claverton Down, Bath BA2 7AY, UK*

<sup>3</sup>*Kavli Institute of Theoretical Physics, University of California Santa Barbara, Santa Barbara, CA 93106*

<sup>4</sup>*Department of Physics, University of California Santa Barbara, Santa Barbara, CA 93106, USA*

<sup>5</sup>*James Franck Institute, The University of Chicago, Chicago, IL 60637, USA*

<sup>6</sup>*Department of Physics, The University of Chicago, Chicago, IL 60637, USA*

<sup>7</sup>*Kadanoff Center for Theoretical Physics, The University of Chicago, Chicago, IL 60637, USA*

(Dated: October 2, 2020)

In this review, we summarize recent progress in understanding the role and relevance of topological excitations in a special category of systems called active matter. Active matter is a class of nonequilibrium systems in which individual constituents convert energy into motion at the microscale. We discuss topological features of active matter ranging from topological defects in symmetry-broken phases to topologically protected wave propagation and non-Hermitian skin modes, emphasizing their distinguishing nonequilibrium properties and experimental ramifications. We first review how the proliferation of self-propelled topological defects in active nematics results in novel collective phases, which can be manipulated by geometry and patterning, and discuss possible implications in biological tissues. We then illustrate how the propagation of waves in active fluids and solids can be dramatically affected by the presence of topological invariants characterizing their dispersion relations. We conclude by pointing out future challenges and prospects, both theoretical and experimental, for this exciting and rapidly growing field.

Topology describes properties that are preserved under continuous deformations. In condensed matter physics, topological defects occur in ordered media [1–8] such as dislocations in crystals, disclination in liquid crystals, or vortices in superfluids. Topology also characterizes topological states such as the quantum Hall effect [9] and topological insulators [10], that are described by discrete invariants rather than an order parameter manifesting a broken symmetry.

Topological defects are distinctive singular textures that are fingerprints of the broken-symmetry field [5, 11]. They are often formed in quenches from the disordered state or when order is frustrated by curvature, external fields, or boundary conditions. In orientationally ordered media, defects are point-like in two dimensions (2D), and both point and line-like in three dimensions (3D). They are labelled by topological invariants measuring the winding of the broken-symmetry variable along a path or on a surface enclosing the disordered defect core. Topological defects constitute elementary excitations of the homogeneous ordered state. When viewed as effective quasiparticles, the statistical mechanics and dynamics of defects offers a dual picture to that of the conventional order parameter [12]. In 2D, the unbinding of defect pairs drives the celebrated Berezinskii-Kosterlitz-Thouless (BKT) phase transition [1–4], which is found in a wide variety of systems [13], ranging from superfluid and superconducting films to planar crystals. The BKT mechanism reveals a distinctive universality class of topological defect-induced continuous phase transitions at equilibrium.

Topological invariants similar to the winding numbers of defects can also be used to characterize the twisted nature of wave propagation in certain materials. The ap-

pearance of such topological structures lies at the heart of states of matter such as topological insulators and superconductors [14–17]. A common feature of these topological materials is that their bulk is an electrical insulator, but they exhibit robust metallic edge or surface states [18] protected by a bulk topological invariant. Because of their topological nature, these edge states do not allow backscattering and hence are immune to disorder and defects, an attractive feature for technological applications [10, 19]. It quickly became clear that such ideas are also applicable to mechanical [20–22], photonic [23, 24] and acoustic waves [25], leading to intense efforts in designing topological metamaterials with robust functionalities.

While most topological phenomena have been explored extensively in passive inanimate materials, their extension to nonequilibrium systems (including, possibly, living matter) remains an open challenge. In the past decade or so, there has been growing interest in developing a framework to quantitatively understand and characterize the physics of materials far from equilibrium. An important class of such materials is provided by active matter [26–28], which describes large interacting collections of individually self-driven units (see Box 1). The constituents in active systems locally consume free energy to execute self-sustained motion or work. The field of active matter is partly motivated by the aim of bringing living systems into the scope of condensed matter physics [29–31], and yet the field now boasts a wide variety of inanimate and synthetic experimental realizations ranging from self-propelled colloids [32, 33] and vibrated grains [34] to robot swarms [35] and reconstituted biofilament suspensions [36, 37]. The large-scale collective and emergent behavior of active systems is of great interest

with broad applicability over a wide range of scales, from bird flocks to the cytoskeleton of a single cell. Active matter shares striking similarities with other kinds of driven-dissipative systems [38, 39] ranging from optics [40] to open quantum systems [41–45], that are however outside the scope of this review.

Active materials are a challenging frontier of nonequilibrium statistical mechanics because of the breakdown of detailed balance and time-reversal symmetry (TRS) [46, 47] at the microscale. A powerful approach is the use of continuum hydrodynamic theories augmented to account for active driving [27]. The primary strategy relies on identifying a small set of so-called hydrodynamic degrees of freedom [48] using the symmetries of the system (broken or otherwise), conservation laws, and relevant order parameters; another possibility is the use of machine learning techniques [49–51]. Models of dynamical critical phenomena [52], pattern formation [53], and fluid mechanics [54] provide the necessary point of departure, liberated from the constraints of equilibrium thermodynamics (see Box 1). This approach has lead to striking theoretical predictions such as the existence of two-dimensional ordered flocks [55, 56], giant number fluctuations [34, 57], spontaneous flow instabilities of active suspensions [58, 59], motility induced phase separation of purely repulsive particles [60, 61], and spontaneous rotation from non-reciprocity [62], along with ambitious applications to cell biology [63–65]. It has now paved the way to descriptions involving active field theories [66].

An important lesson learned from the extensive study of equilibrium matter is that topological tools provide a powerful way of identifying the relevant physical degrees of freedom. This framework complements the conventional hydrodynamic viewpoint and offers a new perspective beyond simple order-disorder scenarios. In this review, we discuss the relevance of topological defects and topologically protected states in active matter. Crucially, topology remains intimately tied to symmetries. When combined with spatial symmetries and spontaneous order, the breaking of TRS at the microscopic scale can lead to broken TRS on large scales, with phenomena such as the spontaneous motion of topological defects [37, 62, 67] and fluid analogues of topological insulators [68–71]. Box 1 reviews the common emergent spatial symmetries that appear in active fluids. Since many active particles are elongated, they can organize into states of orientational order similar to liquid crystals [27]. In addition, *chiral* states can exist in active systems with or without orientational order (polar or nematic) [62, 72–76].

The interplay between broken time-reversal symmetry, orientational order, and topology in active media is the keystone holding together the many physical examples presented in this review. We discuss the role of topological defects in active fluids with either polar or nematic symmetries. Active driving entails defects with autonomous motility, providing a distinct signature of broken TRS. The unbinding and proliferation of ac-

tive defects then mediates nonequilibrium phase transitions [77, 78] leading to lively chaotic flows in active nematics [79]. Collective motion is yet another dramatic manifestation of large scale TRS-breaking [33, 36, 80]. When confined to complex substrates, either as patterned metamaterials [68] or curved surfaces [70], one finds robust topologically protected sound modes in a realization of a Chern insulator in a nonequilibrium fluid. Combining activity with parity violation allows chiral active fluids with topological waves [71] and dissipationless transverse viscosities [74, 76, 81] akin to those in fluids of electrons [82]. A distinct class of topological states in active solids leads to non-Hermitian skin modes, protected by winding numbers characterizing point-gapped Hamiltonians [83–85]. We conclude by summarizing the fascinating role of topological excitations in biology and the emerging prospects for using such ideas to pattern and control synthetic active fluids for technological applications.

## I. TOPOLOGICAL DEFECTS IN ACTIVE MATTER

Just as in equilibrium, defects play an important role in the spatiotemporal dynamics and relaxation of active ordered phases. In this section, we focus primarily on 2D active fluids with orientational order. Polar active fluids, also called Toner-Tu fluids [55, 56, 86, 87], can develop ordered collective motion through spontaneous symmetry breaking, akin to a model of “flying spins”, using an analogy with magnets. In contrast, active nematics [57, 79] are composed of head-tail symmetric rod-like entities that order and exert internally generated stresses on their surroundings. These fluids display no net motion on average because they are apolar, but they combine the rich rheology of liquid crystals with active driving.

While polar fluids with vectorial order parameters exhibit defects such as asters and vortices characterized by integer topological charge, the inversion symmetry of nematic order means the simplest defects are disclinations with half-integer charge (see Box 2). Active ordered fluids have been assembled from a variety of soft materials [33, 36, 37, 88, 89] and display emergent dynamics of topological defects. Asters and vortices have been observed in high-density motility assays [90, 91], confined and membrane-bound reconstituted cortical extracts [88, 89, 92], and suspensions of colloidal rollers motorized by an electric field [93]. Nematic disclinations have also been identified in diverse systems, including cytoskeletal filament-based active nematic suspensions [37, 94–96] and collections of living cells [97–100].

In recent years topological defects have been the focus of intense research, particularly in active nematics [79], which exhibit large scale flows and spatiotemporal chaos through the spontaneous proliferation and motion of topological defects. It is then natural to ask if the resulting dynamical states can be understood from

## Box 1: Models of active fluids.

Active systems composed of self-propelled units that dissipate energy to create motion and forces can exhibit various collective phases that depend on the symmetry of both the interaction and active motion. Aligning active agents can develop polar (vectorial) and apolar (nematic) orientational order. Scalar active particles can undergo motility-induced phase separation. In this case the order parameter is a scalar, i.e., the density difference between the dense and dilute phases. Active particles may also be chiral and organize in states with macroscopic chirality. While polar and nematic chiral states are also possible, they are not shown here for simplicity. In this box, we primarily focus on fluids and will not discuss active solids and other translationally ordered media.

### Active polar fluids

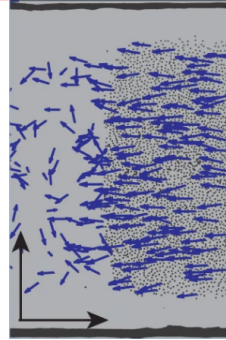
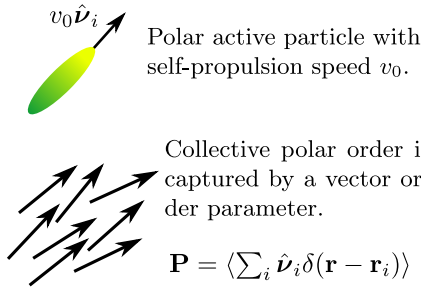


**Fig. B1** Polar fluid composed of colloidal rollers (Ref. [33]).

The hydrodynamics of an active polar fluid on a substrate involves the density field ( $\rho$ ) and the order parameter ( $\mathbf{P}$ ), and is given by the Toner-Tu equations [56].

$$\partial_t \rho + v_0 \nabla \cdot (\rho \mathbf{P}) = 0$$

$$\partial_t \mathbf{P} + \lambda \mathbf{P} \cdot \nabla \mathbf{P} = [a_2 - a_4 |\mathbf{P}|^2] \mathbf{P} + K \nabla^2 \mathbf{P} - \nabla \Pi$$

Both  $v_0$  and  $\lambda$  are active parameters capturing advection, while  $a_2, a_4$  control the ordering transition with  $K$  an elastic constant and a density dependent pressure  $\Pi(\rho)$ .

### Scalar active matter

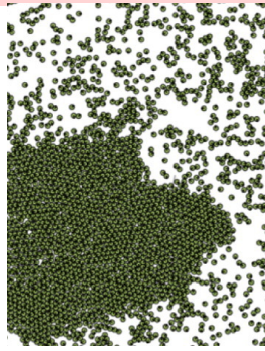
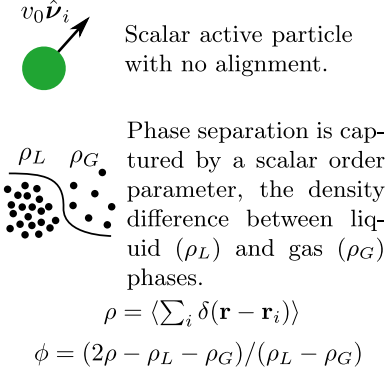


**Fig. B3** Simulation of active particles undergoing MIPS. (Ref. [61])

The simplest continuum model of motility-induced phase separation (MIPS) is of Cahn-Hilliard form involving the density ( $\rho$ ) [60].

$$\partial_t \rho = \nabla \cdot [D(\rho) \nabla \mu]$$

$$\mu = \ln[\rho v(\rho)] + \kappa(\rho) \nabla^2 \rho$$

The effective chemical potential  $\mu$  includes the density suppression of motility  $v(\rho)$  and nonintergrable gradient terms ( $\kappa'(\rho) \neq 0$ ). Density also suppresses the diffusion constant ( $D \propto [v(\rho)]^2$ ).

### Active nematic fluids

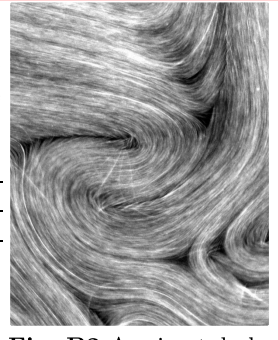
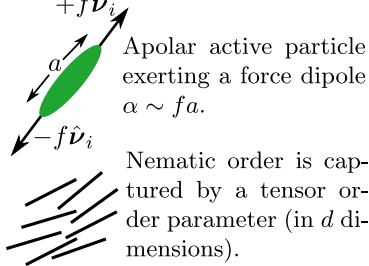


**Fig. B2** A microtubule-kinesin active nematic film (Ref. [37]).

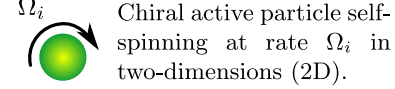
Incompressible active nematics minimally couple nematic order ( $\mathbf{Q}$ ) and flow ( $\mathbf{u}$ ) driven by an active stress ( $\sigma_a = \alpha \mathbf{Q}$ ) [79].

$$\partial_t \mathbf{Q} + \mathbf{u} \cdot \nabla \mathbf{Q} + [\omega, \mathbf{Q}] = \lambda \mathbf{E} + [a_2 - a_4 S^2] \mathbf{Q} + K \nabla^2 \mathbf{Q}$$

$$\eta \nabla^2 \mathbf{u} - \Gamma \mathbf{u} + \nabla \cdot \sigma_a - \nabla \Pi = \mathbf{0} \quad \nabla \cdot \mathbf{u} = 0$$

Force balance involves both friction ( $\Gamma$ ) and viscosity ( $\eta$ ).  $\mathbf{E}$  and  $\omega$  are symmetric and antisymmetric parts of  $\nabla \mathbf{u}$  causing flow alignment ( $\lambda$ ). Nematic ordering [ $S^2 = \text{tr}(\mathbf{Q}^2)d/(d-1)$ ] is controlled by  $a_2, a_4$  and the elastic constant  $K$ .

### Chiral active fluids



Collective chirality is captured by a scalar field, the intrinsic rotation frequency.

The simplest hydrodynamics of an isotropic chiral active fluid in 2D includes density ( $\rho$ ), flow ( $\mathbf{u}$ ) and the internal spin density ( $\Omega$ ) [74,81].

$$\partial_t \rho + \nabla \cdot (\rho \mathbf{u}) = 0$$

$$\partial_t \mathbf{u} = \eta \nabla^2 \mathbf{u} - \Gamma \mathbf{u} + \eta_R \nabla_{\perp} (2\Omega - \omega) + \eta_o \nabla^2 \mathbf{u}_{\perp} - \nabla \Pi$$

$$\partial_t \Omega = \tau_0 - \Gamma_{\Omega} \Omega - 2\eta_R (2\Omega - \omega) + D_{\Omega} \nabla^2 \Omega$$

Along with regular viscosity ( $\eta$ ) and friction ( $\Gamma$ ), we also have odd viscosity ( $\eta_o$ ) and rotational viscosity ( $\eta_R$ ), the latter in the antisymmetric stress. Chirality enters through terms involving  $\mathbf{u}_{\perp} = \hat{\mathbf{z}} \times \mathbf{u}$  and the vorticity  $\omega = \hat{\mathbf{z}} \cdot (\nabla \times \mathbf{u})$ . The active torque ( $\tau_0$ ) injects spin which is damped by spin friction ( $\Gamma_{\Omega}$ ) and diffusion ( $D_{\Omega}$ ).



**Fig. B4** Chiral fluid of colloidal spinning magnets (Ref. [76]).

the perspective of defect unbinding, and if the equilibrium BKT transition can be extended to the active realm. Defects also offer natural nonlinear stable patterns than can be used to control, localize and channel stresses and flows, even in biological tissues. These subjects will be the focus of the rest of this section.

### A. Active defects spontaneously move

One of the distinguishing aspects of defects in active matter is their capacity for spontaneous and autonomous motion. The large distortions of the order parameter around a topological defect generate active stresses, which can lead to a local directed current due to the absence of detailed balance. The nature and symmetry of the local currents depends on the defect geometry. In particular, in active nematics, the net current vanishes by symmetry at the core of  $-1/2$  defects, but is finite at the core of  $+1/2$  defects. As a result, by virtue of its local geometric polarity, the comet-shaped  $+1/2$  disclination (see Box 2) acquires intrinsic self-propulsion through self-induced active flows [67]. The direction of motion of the defect is determined by its local orientation and by the sign of the active forcing. In extensile fluids  $+1/2$  defects actively propel themselves along the head of the comet, while in contractile system the active propulsion is directed along the comet's tail. On the other hand, by virtue of their threefold symmetry, disclinations of charge  $-1/2$  are not intrinsically self-propelled (see Box 2). If chiral active stresses are present,  $+1/2$  disclinations self-propel at an angle relative to their polarity [75, 101], and intrinsic active spinning renders defect trajectories circular [75]. In polar fluids, charge  $+1$  spiral vortices undergo spontaneous rotation [102] due to the chirality of their spiral texture. Other low charge defects, such as circularly symmetric asters and antivortices, perform neither rotational nor translational spontaneous motion. In contrast to defect motion in externally driven systems, the motion of active defects is dictated by the local *geometry* of the defect itself and not by a fixed external field, as would be the case, for example, for driven vortices in a superconducting film. This profound distinction leads to a plethora of phenomena characteristic of active matter.

Defects can also occur in 3D active suspensions, but they are less well understood. Bulk active nematics are susceptible to a generic hydrodynamic instability [58] that spontaneously generates individual disclination loops [103–105]. Unlike in 2D, where opposite charge defects are topologically constrained to be created and annihilated in pairs, charge neutral disclination loops [6] in 3D can be nucleated on their own. The active flows caused by the director distortion around a disclination loop cause it to stretch, twist, and buckle [105]. The complex configurational dynamics of these loops combined with topological reconnections leads to chaotic 3D flows, that have been recently observed in simulations [103] and experiments [104]. Recent theoretical

work has also extended similar ideas to chiral phases such as bulk active cholesterics. Here defects in the cholesteric pitch ( $\lambda$ -lines) [106] and nonsingular topological textures such as half-skyrmions or merons [107], though not self-propelled, can sustain coherent rotations and steady defect patterns along with spatio-temporal chaotic flows.

### B. Defect dynamics, unbinding and ordering out of equilibrium

From a fundamental point of view, defect motility raises intriguing possibilities for phase transitions. The consequences of self-propelled defects have been explored predominantly in 2D active nematics [67, 77, 78, 108–110]. The defect-driven chaotic flows lead to a state dubbed “active turbulence” [110, 111], which is characterized by vorticity and shear flows on a typical length scale that controls the mean defect separation and is set by a balance of active and elastic stresses [110, 112–114]. The phenomenology of active turbulence in nematic fluids has been detailed in a recent review [79]. Here we focus more on its topological aspects and sketch the physical arguments underpinning the unbinding of active defects [77].

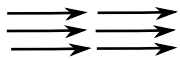
At equilibrium, defects in 2D behave as point charges that interact via a Coulomb potential. This pair interaction is mediated by the underlying elasticity of the ordered fluid and scales as  $K \ln(r/a)$ , where  $K$  is an elastic stiffness,  $r$  is the pair separation and  $a$  the defect core size (see Box 2). The equilibrium BKT transition then occurs at a finite temperature beyond which entropic effects overwhelm the elastic energy, allowing defect pairs to unbind and proliferate, thereby disordering the system. In a 2D *active* nematic, an isolated  $\pm 1/2$  disclination pair continues to experience the passive attractive force  $\sim K/r$  from elasticity, but in addition, the  $+1/2$  defect can propel itself with speed  $\sim v_0$  away from the  $-1/2$  defect. The balance of elastic and active forces sets a length scale  $r_c \sim K/v_0$ , beyond which activity always rips apart the defect pair, causing it to inevitably unbind. This simple picture is spoiled by the presence of rotational noise ( $D_R$ ) in the direction of motion of the  $+1/2$  defect. As the system is active, the motility of the  $+1/2$  disclination is determined by its local geometry, and not by an external field as in a driven system. As a result, the  $+1/2$  defect has a finite *persistence length*  $\ell_p = v_0/D_R$  beyond which its motion is not ballistic. Comparing the two length scales we get a simple criterion for active defect unbinding [77] occurring when  $\ell_p > r_c$ . Note that rotational noise here stabilizes the quasi-ordered nematic phase below a finite activity threshold by disrupting the persistent motion of the  $+1/2$  defect. This order-from-disorder mechanism highlights the difference between active and driven defects: the latter would inevitably unbind.

The interacting gas of unbound and swarming defects provides a useful picture to describe the state of

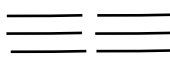
## Box 2: Topological defects in passive and active ordered fluids.

Topological defects are special zeros of the order parameter field. They are point-like in 2D liquid-crystalline media and are classified by their winding number or topological charge  $s = \Delta\Theta/2\pi$ , where  $\Delta\Theta$  is the net angle through which the order parameter rotates as one encircles the defect. The charge  $s$  is positive if the order parameter rotates in the same direction as the path traversed, negative if it rotates in the opposite direction. In a 2D XY magnet where the order parameter is a vector field, the lowest charge topological defects are asters and vortices (both with  $s = +1$ ), and anti-vortices or cross-hairs (with  $s = -1$ ). In a nematic film, where the broken symmetry identifies only orientation (not direction) and the order parameter is a line field, the lowest energy defects are disclinations of strength  $s = \pm 1/2$ .

Polar order: Vector field

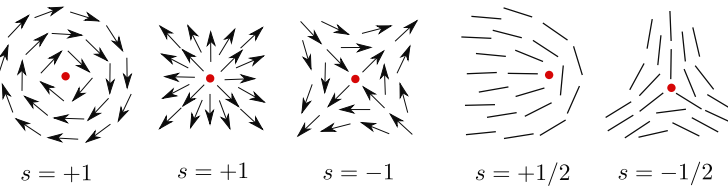
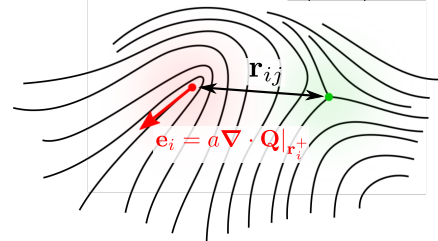


Nematic order: Line field

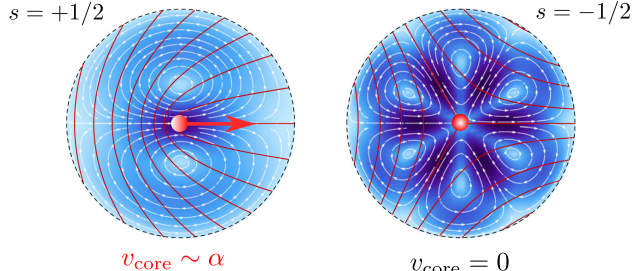


In 2D passive liquid crystals, two defects of strength  $s_i$  and  $s_j$  and separation  $\mathbf{r}_{ij}$  interact via a Coulomb potential, mediated by nematic elasticity ( $K$ ) and cutoff by the defect core size ( $a$ ).

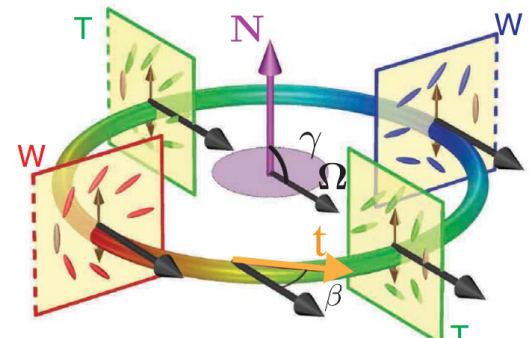
$$V(\mathbf{r}_{ij}) = 2\pi K s_i s_j \ln\left(\frac{|\mathbf{r}_{ij}|}{a}\right)$$



In 2D *active* nematics, defects behave like quasiparticles “dressed” by the active flows they produce [77,79]. The flow generated by a  $+1/2$  defect is finite at the core, rendering the defect a self-propelled particle with a well-defined polarization ( $\mathbf{e}_i$ ). On the other hand, the flow generated by a  $-1/2$  defect vanishes at the core. To leading order in activity, defects interact via the same Coulomb force as in the passive case but also exert active torques on each other. Defects in active nematics therefore behave as an interacting mixture of active ( $+1/2$ ) and passive ( $-1/2$ ) charged quasiparticles [77].



The flow  $\mathbf{u}$  generated by a defect is obtained by solving the Stokes equation that balances active stresses of strength  $\alpha$  due to a defect texture described by the nematic order parameter  $\mathbf{Q}$  with frictional and viscous damping [67,109] (also see Box 1).



Bulk active nematics support topologically neutral disclination loops that smoothly interpolate  $+1/2$  and  $-1/2$  defect textures in local cross-sections of the loop. The  $\pm 1/2$  wedges are equivalent in 3D by escape into the third dimension. The simplest of such wedge-twist loops is characterized by a rotation vector ( $\Omega$ ) in the plane of the loop ( $\gamma = \pi/2$ ), making an angle  $\beta$  with the local tangent ( $\mathbf{t}$ ). Similar to their 2D counterparts, the local active flows generated by such disclination loops drive complex dynamics in 3D bulk active nematics [104].

active turbulence. Several models of varying complexity have been proposed for the dynamics of active defects [67, 77, 94, 109, 115–119]. While details differ, the basic physics is the same. Recent work has also emphasized the non-reciprocal nature of active defect interactions [119, 120], a feature that remains to be explored. Coarse-graining over many defects allows a hydrodynamic description of the active defect gas [78],

along the lines of previous classic works in the context of superfluid vortices [121] and 2D crystal melting [122]. Importantly, a hydrodynamic treatment of defects offers a theoretical handle on the strongly interacting many-body dynamics of this far-from-equilibrium system. As a crucial ingredient, this description includes a polarization field that captures the average orientation of a collection of active  $+1/2$  defects. This field

accounts not only for self-propulsion actively driving material flow, but being a vector, the orientation also experiences active torques. When activity is sufficiently strong, one finds that the  $+1/2$  defects spontaneously condense into a polar-ordered collectively moving state—a defect flock [78]. The fleeting defects constantly turn over due to creation and annihilation events, but polar order persists for infinitely longer than the individual defect lifetime. Heuristically, such a state arises when the underlying nematic elasticity is too slow to relax the distortion created in the wake of an unbinding defect pair. Similar defect-ordered states have been observed previously in simulations, either with polar ordering [123–126] or defect lattices [127]. Experiments on microtubule-kinesin based active nematic films have reported an extraordinary *nematic* ordered defect state [123]. While continuum simulations recover largely transient nematic defect ordering [125, 128], this observation continues to be a theoretical puzzle. Recent work suggests elastic torques may play a role in antipolar ordering of defects [129, 130].

Finally, vortex unbinding has been shown to also play a role in disordered polar active fluids [131]. Here, active flows conspire with quenched obstacles to realize a dynamical vortex glass that can be rationalized through an effective Kosterlitz-Thouless-like argument in analogy with dirty superconductors. Generalizing similar ideas to active matter in heterogeneous environments [132] remains an open question.

### C. Active defects under confinement

The spontaneous motion of active defects offers new avenues to rectify and control chaotic flows. A direct way is through confinement. Active nematic films, which are built by depleting microtubule bundles and kinesin motor complexes onto an oil-water interface [37], have emerged as a versatile platform to manipulate defects using confinement. One simple approach is through a viscous contrast in the fluid contacting the nematic film that hydrodynamically constrains flow [137]. More structured environments, such as bulk smectics [113, 138], can be controlled by external fields and patterned with defects. When in contact with the active nematic layer, focal conic domains in the smectic, for instance, cause the active disclinations to swirl along circular trajectories [113]. This provides a neat way to rapidly reconfigure and channel flows in the system by rectifying defect motion.

Physical confinement has also been studied, particularly in the disc geometry. Microtubule-based active nematics develop steady circulating flow when strongly confined, giving way to a pair of  $+1/2$  defects (as topologically required) nucleating at the boundary and orbiting around each other [133, 139]. For large disc sizes, more defects nucleate and unbind in the bulk, degenerating into active turbulence (Fig. 1a). Laterally confined nematics support shear states into which  $+1/2$  defects are

continually injected, as they swim around each other in a dancing fashion [140, 141]. While experiments and continuum simulations agree well in many regards, recent work has noted discrepancies in predictions related to defect nucleation and steady flow states in confined nematics [133], suggesting more theoretical work is required. Polar fluids of colloidal rollers generate large inhomogeneous vortex patterns when confined [93], though defects do not proliferate upon deconfining. Instead spontaneous flow and substrate disorder can pattern a synthetic gauge field [131] that creates and spatially pins such defects (Fig. 1c).

A third way is to confine active fluids using curved substrates. Curvature frustrates order and often necessitates defects [12], providing an exciting avenue to pattern active fluids. Active nematics assembled onto spherical vesicles (Fig. 1b) exhibit spontaneous cell-like shape oscillations driven by the periodic dynamics of four active  $+1/2$  defects [94]. On a torus, the spatially varying positive and negative Gaussian curvature causes defects to unbind, attracting disclinations to regions of matching sign curvature [95], thereby filtering them by charge. Polar fluids on a sphere form vortices at the poles and a distinctive polar band that concentrates near the equator as a result of active advective fluxes pushing material towards the equator [70, 142].

### D. Biological relevance of topological defects

One of the most exciting developments has been the recent characterization of topological defects in living tissues and cellular assemblies viewed as active materials. Elongated cells can form ordered liquid crystalline textures interrupted by  $\pm 1/2$  disclinations. In confluent epithelial tissues [99] and dense cultures of neural progenitors [100], cells were found to preferentially migrate and accumulate at  $+1/2$  disclinations and escape from  $-1/2$  disclinations (Fig. 1e). The large distortion of order around the defect generates strong local active stresses (Fig. 1f) that have been correlated with cell extrusion and death in epithelia [99]. Similar phenomena have now been reported in other systems as well, such as mound formation and buckling at  $-1/2$  defects in bacterial biofilms [143], multilayers and cavities seeded by  $\pm 1/2$  disclinations respectively in myxobacteria colonies [144] and more recently in the context of developing Hydra [145], where topological defects in aligned supracellular actomyosin drive morphogenesis of the regenerating tissue. Beyond nematic disclinations,  $+1$  defects have also been recently identified in confined cell monolayers to provide sites for growth and cellular differentiation [146, 147], suggesting defects may play a wider role in organizing tissue morphogenesis.

Active defects have also been theoretically found to control the dynamic morphologies of growing bacterial colonies [148] and shape-shifting active shells [149]. On a more subcellular level, the mitotic spindle provides a

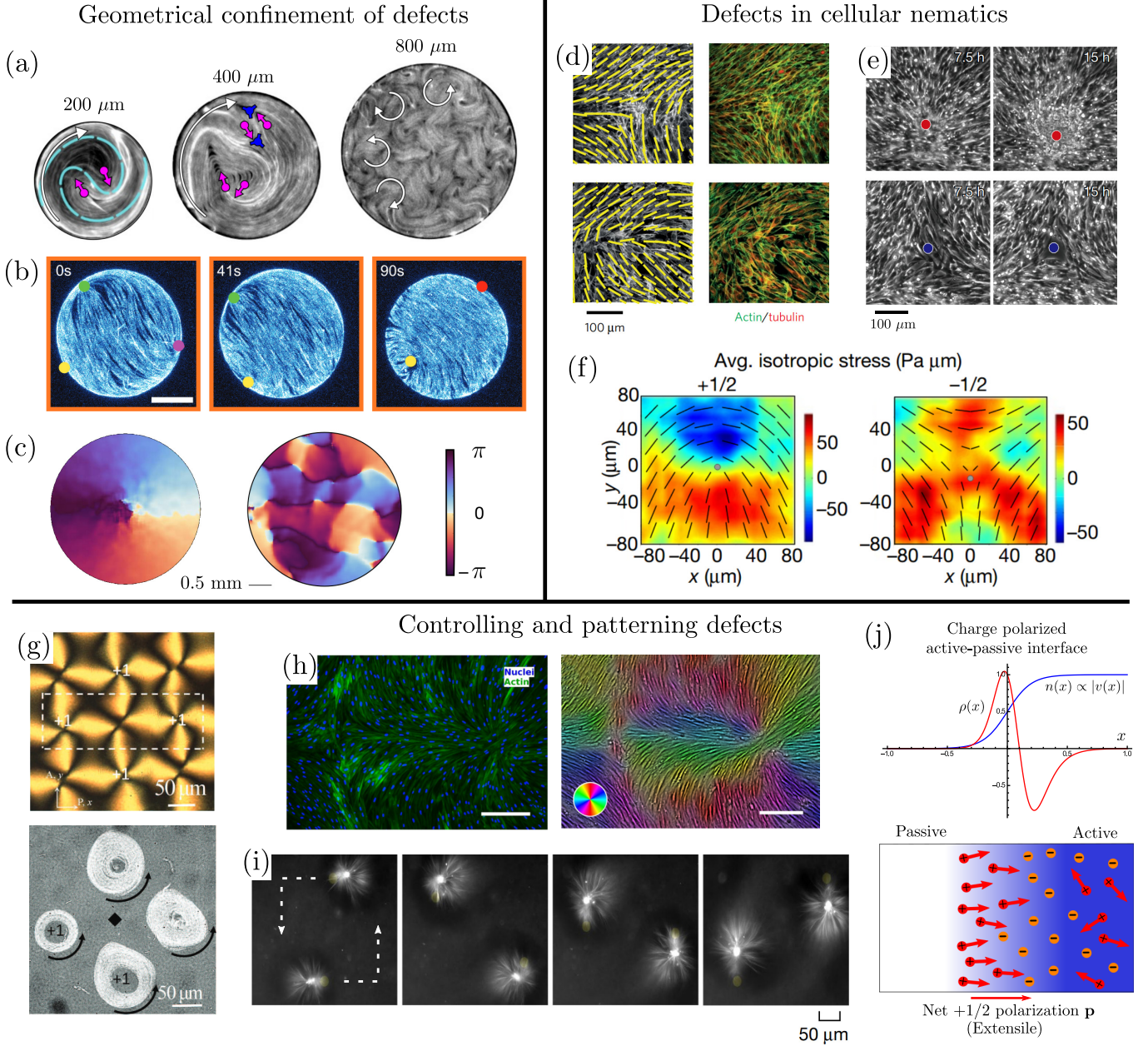


FIG. 1. *Geometrical confinement of defects:* (a) Circulating +1/2 defects in a microtubule-kinesin active nematic film confined to a disc (200 μm), with more pairs of defects unbinding to create turbulent flows for large disc diameters (800 μm) [133]; (b) The same system now condensed onto a spherical vesicle (scale bar, 20 μm) exhibits periodic oscillations of the four +1/2 defects present [94]; (c) Schlieren texture of a colloidal polar fluid in a disc geometry displaying a system-spanning vortex (left) and a pattern of pinned vortex-antivortex pairs (right) induced by randomly located obstacles [131]. *Defects in cellular nematics:* (d) Active ±1/2 disclinations have been identified in aligned populations of spindle-shaped mouse fibroblasts [97]; (e) Cells accumulate (deplete) at the cores of +1/2 (−1/2) defects, the former seeding mound formation in dense monolayers of neural progenitor cells [100]; (f) Similar defects in epithelial monolayers of MDCK cells generate large compressive stresses (in blue) only at the head of +1/2 disclinations that locally trigger cell extrusion and apoptosis [99]. *Controlling and patterning defects:* (g) Directing polar flows of bacteria dispersed in a nontoxic liquid crystal patterned with an array of +1 defects [134]; (h) Patterning a tissue of human fibroblast cells (HDF) growing on a liquid crystal elastomer with a predesigned texture of ±1 defects (scale bar, 300 μm) [135]; (i) Time-series of dynamically assembled asters transported along a predetermined trajectory within a bulk microtubule-kinesin suspension, by local light activation [136]; (j) An active-passive interface in an active nematic hosts a spatially polarized topological charge density ( $\rho$ ) with preferentially oriented +1/2 defects, while the total defect density ( $n$ ) is higher on the active side [78].

classic example of a self-organized aster-like defect maintained in constant flux by actin treadmilling and motor activity [150]. Separate from the above, recent *in-vivo* experiments on starfish oocytes also demonstrate excitable biochemical spiral waves and defect chaos in the expression of certain membrane bound signalling proteins [151]. While it remains to be seen what the full implications of topological defects to biology are, it is clear that such an approach is highly productive and at the frontier of active matter research.

### E. Experimental advances and defect-based control of active matter

Beyond elucidating novel phenomena in nonequilibrium physics lies the challenge of harnessing and controlling it. Active matter experiments have made rapid strides in the past decade and are now poised to engineer reconfigurable and programmable materials. A key strategy is to use topological defects as natural motifs to build dynamic structures with organized flow. Biocompatible liquid crystals perfused with swimming bacteria afford simple static control through prepatterned topological defects (Fig. 1g) that capture bacteria and direct their collective motion based on topological charge [134, 152]. A related strategy has also been employed more recently to pattern defects in aligned epithelial monolayers (Fig. 1h) grown on structured substrates with strong anchoring [135, 153].

Modern advances in engineering optical control of biomolecular activity provide a platform to dynamically control and pattern active materials at will [136, 154, 155]. This has been demonstrated in microtubule-kinesin based gels [136], where local light activation reversibly self-assembles 3D asters dynamically stabilized by the clustering and polarized motion of motor proteins. These defect structures can be moved and arranged in arbitrary patterns in both space and time (Fig. 1i). A similar strategy has also been employed recently in active nematic films to locally pattern active stresses and direct defect motion using spatio-temporal activity gradients [155]. Inhomogeneous activity profiles can act as “electric fields” and drive the sorting of defects by topological charge [78], primarily due to the self-propulsion of  $+1/2$  disclinations which accumulate in regions of low activity, unlike nonmotile  $-1/2$  disclinations (Fig. 1j). This can be exploited to create defect patterns in active fluids and concomitantly design functional materials with targeted transport capabilities. Evidently, defect-based control is poised to create innovative active metamaterials in the future [155, 156], possibly facilitated by machine learning algorithms [49].

## II. TOPOLOGICAL BAND STRUCTURES IN ACTIVE MATTER

In this section, we review how topological concepts characterize propagating waves in active fluids and solids, with a particular focus on continuum hydrodynamic theories. We survey how the active fluids reviewed in Box 1 and corresponding active solids can be harnessed to realize topological edge states. Here, the topology is contained in the dispersion relation and the normal modes of the waves, that we collectively refer to as the band structure of the active medium. At the heart of topological wave propagation lies the principle of *bulk-boundary correspondence* that guarantees the presence of peculiar states at boundaries and interfaces (such as chiral edge states robust against defects and disorder) because of a topological invariant characterizing the bulk of the medium. Intuitively, the discrete topological invariant must change at the edge of the system (or at any interface between topologically distinct states). This change is only possible if the invariants become ill-defined at the interface: this requires that a gap closes, leading to the existence of states at the frequencies in which bulk propagation is forbidden. This principle allows us to determine behavior at the edge by calculating an invariant from bulk physics.

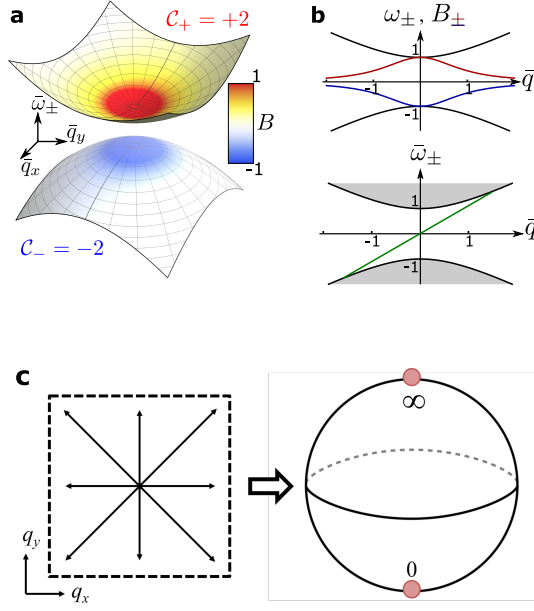
We will discuss two broad classes of topological phenomena: topological wave propagation, and non-Hermitian skin effects. In topological wave propagation, activity is either ultimately responsible for the existence of topological states, or substantially affects their properties. These states arise in Hermitian systems, are akin to electronic topological insulators and, crucially, are characterized by the same topological invariants. Nonetheless, activity plays a crucial role in soft and biological matter, in which all motion is overdamped at small scales: overdamped wave propagation can only occur in *active* fluids and solids. Non-Hermitian skin effects are a class of topological phenomena unique to nonequilibrium systems, in which the matrices describing the wave propagation become non-Hermitian, and in which all the bulk eigenstates of these matrices become localized at the boundary of finite systems. This situation attracted a lot of attention in the context of driven-dissipative quantum systems [38, 157–160], and is also related to the presence of bulk topological invariants, characterizing so-called point-gapped Hamiltonians [83, 84] (see Box 4). This situation occurs naturally in active systems in which energy is constantly injected and dissipated, and was demonstrated in active solids [85, 161, 162] and fluids [163].

### A. Active media as topological insulators

Topological invariants in wave propagation can be understood via a simple analogy. When the intrinsic (Gaussian) curvature of a toroid is integrated over the entire

### Box 3: A primer on topological band theory.

In reciprocal space, topological invariants can be defined using the global structure of bands [14,16,17], which are smooth functions of wavevector  $\mathbf{q}$  (see Fig. a). Here we focus on topological aspects of eigenvectors in Hermitian matrices. Consider the linear operator  $L$  that describes wave propagation. Upon solving the eigenproblem with periodic boundary conditions, we obtain the set of normal modes as complex eigenvectors in reciprocal space. These eigenvectors in a given band provide a basis at each  $\mathbf{q}$  to decompose any wave excitation. This framed basis transforms and rotates as we traverse a path in reciprocal space, which is captured by the geometric notion of parallel transport.



The geometry is quantified by defining the so-called Berry connection  $\mathcal{A}_n(\mathbf{q})$  for band  $n$ , which in the simplest setting of a Hermitian operator is given by

$$\mathcal{A}_n(\mathbf{q}) = i [\mathbf{u}_n(\mathbf{q})]^\dagger \cdot [\nabla_{\mathbf{q}} \mathbf{u}_n(\mathbf{q})] ,$$

where  $\mathbf{u}_n(\mathbf{q})$  are the complex eigenvectors with  $\dagger$  denoting complex conjugate and the dot product is over eigenvector components. The curl of this connection gives the Berry curvature, which quantifies how much the eigenvectors rotate and twist to get back to themselves upon completing a closed circuit:

$$\mathcal{B}_n(\mathbf{q}) = \nabla_{\mathbf{q}} \times \mathcal{A}_n(\mathbf{q}) .$$

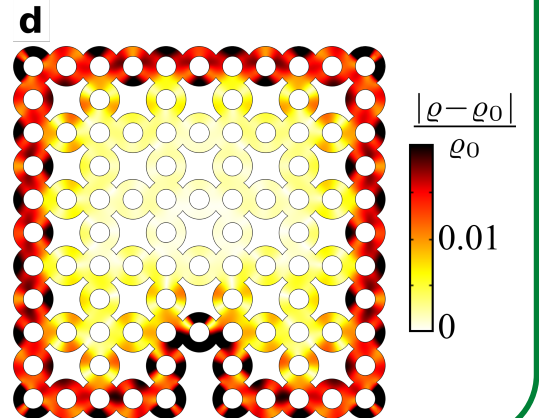
Analogous to the Gauss-Bonnet theorem, we can integrate the Berry curvature over  $\mathbf{q}$  to obtain a topological invariant called the Chern number,

$$C_n = \frac{1}{2\pi} \int d\mathbf{q} \mathcal{B}_n(\mathbf{q}) .$$

The color in Fig. a shows the local Berry curvature  $\mathcal{B}_{\pm}$  for the two bands of a chiral active fluid [71]. Whereas  $\mathcal{A}_n(\mathbf{q})$  and  $\mathcal{B}_n(\mathbf{q})$  are geometric quantities that depend explicitly on  $\mathbf{q}$ ,  $C_n$  is a topological quantity characterizing the band structure as a whole.

There are several key assumptions necessary to make a Chern number  $C_n$  a well-defined integer. First, the reciprocal space must be a closed surface, which is automatically true in periodic lattices that have a Brillouin zone (in which case the reciprocal space, but not necessarily the band structure, has the topology of a torus).

In continuum fluids with no underlying periodic structure, reciprocal space must be compactified explicitly at  $|\mathbf{q}| \rightarrow \infty$  (Fig. c), which can be achieved through regularizing terms such as odd viscosity in chiral active fluids [71]. Another key assumption is that the Berry connection, and therefore the band structure, must be smooth. If two bands touch, then at the point of degeneracy the Berry connection and the Berry curvature are no longer well defined and the Chern number ceases to exist. Therefore, to define the topological invariant, the band structure must be gapped. With these assumptions, bulk-boundary correspondence dictates that the change in Chern number across a boundary or interface counts the number of edge states spanning this gap. An example of the edge state dispersion in a chiral active fluid is plotted in green in Fig. b. One such edge mode is shown in Fig. d for a different system of a topological active-fluid metamaterial [68].



surface, the result must always equal zero, independent of the precise shape. This demonstrates that any toroid can be flattened without tearing (i.e., it is topologically equivalent to a square with opposing sides identified). This is an example of the Gauss-Bonnet theorem [166], which relates the integrated Gaussian curvature of a closed two-dimensional surface to the number of holes in the surface (its genus). This powerful theorem allows us

to calculate global topological features of a smooth surface from purely *local* geometric quantities. Heuristically, the topological invariants of band structures are similar quantities: they are obtained by integrating an abstract curvature describing the geometry of the normal modes of a matrix describing how the wave propagates, as we detail in Box 3.

The key consequence of topological band structures

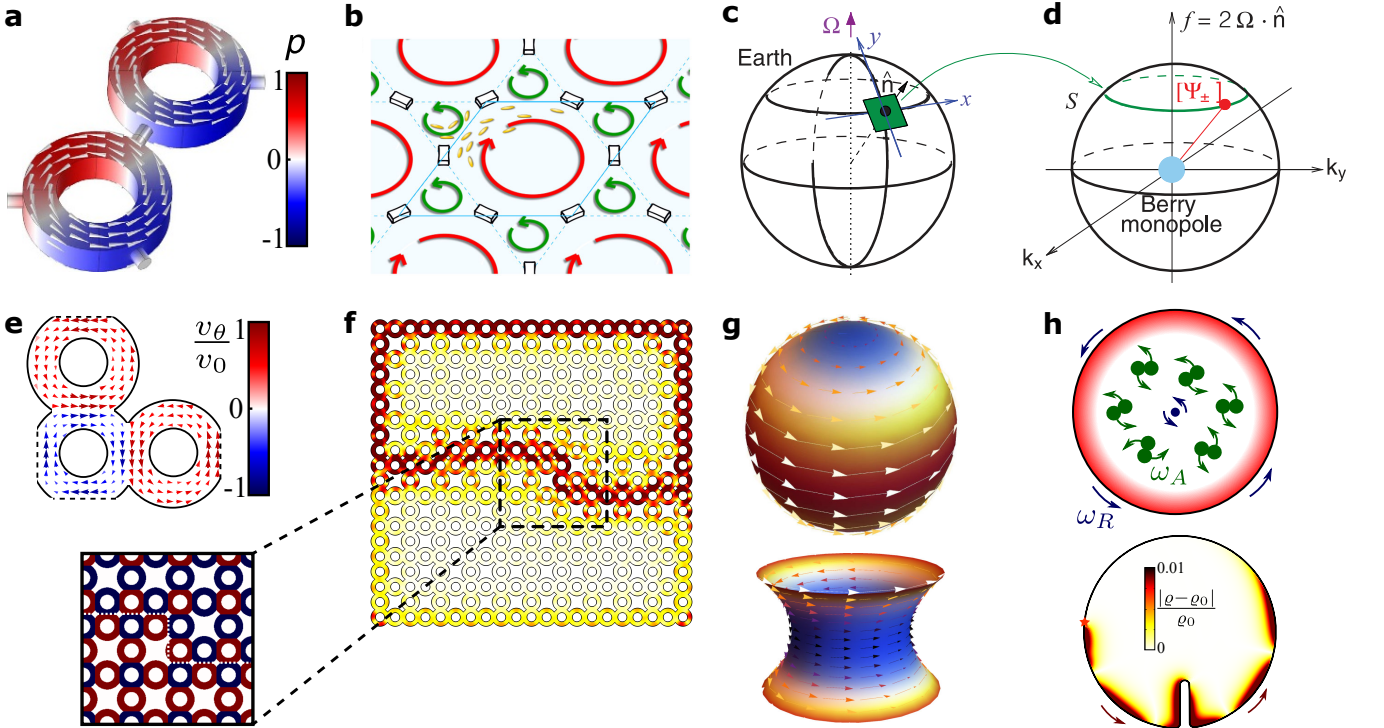


FIG. 2. Topological edge states in fluids far from equilibrium. (a) A topological material based on air driven within circulators in which each unit cell has a net vorticity [164]. (b) A polar active fluid with topological edge states but no net vorticity per unit cell [165]. (c–d) Topological waves on the scale of the Earth in which the equator serves as a boundary along which geophysical waves are topologically protected by a Berry monopole due to the Earth’s overall rotation [69]. (e–f) Phenomenology of topological edge states in a polar active fluid confined inside a Lieb lattice of annuli [68]. Steady state flow (e) and topological density excitations at edges and interfaces of the lattice (f) are shown. (g) Such topologically protected states arise at the equator in a polar active flock confined to the surface of either a sphere (top) or a catenoid (bottom) [70]. (h) Odd viscosity in a chiral active fluid leads to a topologically protected band structure (see Box 3), resulting in topological edge states in a fluid without polar order [71].

is the presence of topologically protected modes at the boundary of a finite sample, or at the interfaces between systems with topologically distinct band structures. In the cases that we consider here (Chern insulators), unidirectional propagation occurs along the edges, for waves with a frequency within a bulk spectral gap in the band structure. Furthermore, these states exhibit topological protection: even if defects, obstacles, or sharp features such as corners are present along the boundary, the waves propagate unabated through and around these obstructions in a robust fashion and without backscattering.

Topological wave propagation can occur in systems such as coupled oscillators [20, 21, 167] as well as simple fluids in circulator arrays [164, 168]. Similar consequences can be achieved by harnessing active components to induce the topology. As an example, a topological solid can be realized by connecting motorized gyroscopes with springs [169–171]. The combination of the rotation of the gyroscopes and the geometry of the lattice breaks TRS, and leads to a mechanical Chern insulator with chiral edge states at its boundary, which persist even when some of the gyroscopes are removed or immobilized. In the next subsections, we illustrate the occurrence of topo-

logical waves in two classes of active fluids: polar active fluids composed of self-propelled particles and chiral active fluids composed of self-rotating particles.

## B. Topological states in confined polar active fluids

Polar fluids naturally break TRS through spontaneous flow, which can be rectified by geometric confinement to realize emergent chirality and novel topological edge states. We begin with the example from Ref. [68] of a polar active fluid confined in periodic microfluidic channels (see Fig. 2e–f). The channel geometry is composed of coupled rings, each reminiscent of an acoustic ring resonator [172] (Fig. 2a). Although the fluid itself is polar and achiral, the annular confinement endows the fluid with a chirality based on either clockwise (CW) or counterclockwise (CCW) flow [33]. For a periodic geometry of rings positioned on a square lattice, an equal number of CW and CCW rings leads to a restoration of time-reversal symmetry in combination with lattice translation. By contrast, removing a single ring from a  $2 \times 2$  super cell of the square lattice results in a so-called Lieb

lattice that breaks time-reversal symmetry on the scale of the unit cell (Fig. 2e).

This symmetry difference between the square and the Lieb lattice imprints on the character of density waves. While the square lattice has band structure degeneracies protected by the presence of TRS, TRS is broken in the Lieb lattice and consequently band gaps open up between non-crossing bands [68]. Each of these gapped bands can be assigned a Chern number,  $\mathcal{C}_n$ , whose value is generically nonzero (see definition in Box 3) and controlled by both the chirality of the flow and the geometry of the lattice. In the limit in which the speed of flow  $v$  is smaller than the speed of sound  $c$ , the penetration depth for the localized mode scales as  $ca/v$  (where  $a$  is the lattice spacing), approaching  $a$  if  $v \approx c$  [68]. In contrast to driven fluids, where achieving this condition requires moderate to high Mach numbers, active fluids afford independent control of flow and sound speed, both of which are typically of the same order in experimental realizations [33, 173]. This naturally leads to well localized edge modes. Recent work has also pointed out that other periodic structures can support edge states even in the absence of net unit cell vorticity [165].

Interestingly, active fluids can allow for wide control of the penetration depth of edge states [68] compared to externally driven fluids [164, 168] in which the speed of the fluid cannot easily exceed the speed of sound. This feature may be technologically advantageous in the design of miniaturized sonic waveguides [68, 174, 175].

As an alternative to periodic confinement, substrate curvature offers a distinct setting which supports topological edge states in polar active fluids [70] (Fig. 2g). Gaussian curvature coupled with mean flow breaks Galilean invariance and generically gaps long wavelength sound modes that acquire a topological character due to the absence of TRS. On the surface of a sphere, a polar active fluid spontaneously circulates around the equator in a chiral fashion [70, 142], experiencing an active analog of the Coriolis force that changes sign across (and vanishes at) the equator. Passive fluids on a rotating sphere, common in geophysical and atmospheric contexts, also exhibit well-known equatorially localized topological sound modes [69] due to the inertial Coriolis force (Fig. 2c-d). In both cases, the equator acts as a gapless interface between two topologically distinct hemispheres. As a result, density waves in a polar active fluid on a spherical surface exhibit unidirectional propagation and topological protection along the equator along which the polar fluid flows [70]. This phenomenon is generic to active flow on any surface with nonzero Gaussian curvature leading to long-wavelength topological sound modes localizing to geodesics that coincide with flow streamlines (Fig. 2g).

### C. Odd viscosity and topological waves in chiral active fluids

In the above examples of polar active fluids, band-structure topology emerges from the spatial environment which the fluid inhabits. Activity primarily serves to break time-reversal symmetry that allows for non-zero Chern numbers. On the other hand, chiral active fluids exhibit topological states even in the absence of structured confinement (Ref. [71] and Fig. 2h). Instead, activity itself endows the fluid with chirality and mesoscopic lengthscales, leading to protected edge states.

For topological states in chiral fluids, activity needs to simultaneously play two distinct roles: (1) breaking time-reversal symmetry and (2) creating a mesoscopic length-scale in the fluid response. Consider a bulk chiral active fluid inside a disk. The fluid will spontaneously rotate due to the balance between local torques arising from self-rotating constituents and dissipation, with rigid-body rotation (having angular velocity  $\omega_B$ ) being the preferred steady state over a broad parameter range [71, 76, 176] (also see Box 1). This rigid-body rotation not only breaks time-reversal symmetry due to flow, but also opens up a zero-frequency band gap in the fluid bulk. The origin of the band gap is rooted in a fundamental symmetry of classical hydrodynamics: Galilean invariance, i.e., constant boosts in velocity leave the system unchanged. Rigid-body rotation breaks Galilean invariance by having a fixed rotation axis and allows the presence of a band gap. While polar fluids required confinement to generate rotation [68, 70, 93], active chiral fluids do so intrinsically in the bulk [71, 76, 176].

To define a topological invariant, the singular behavior of the band structure at large wavevectors (i.e., short lengthscales) must be regularized [71, 177–179] (see Box 3). To do so, the hydrodynamic theory must include higher-derivative terms that lead to high- $\mathbf{q}$  components of the band structure. In a fluid composed of active rotors, an exotic dissipationless response called odd viscosity ( $\eta_o$ , Box 1) acts as such a regularizing term [68, 71, 76, 179, 180]. Nonzero odd viscosity allows all of the high- $\mathbf{q}$  points to be identified with one another, thereby compactifying the entire plane of wavevectors onto a sphere. As in the stereographic projection, the  $|\mathbf{q}| \rightarrow \infty$  limit maps onto a single point (see Box 3). Once compactified, the Chern number can be computed to be  $\mathcal{C} = \text{sign}(\omega_B) + \text{sign}(\eta_o)$  [71]. A striking feature unique to chiral active fluids is that the Chern number can change without closing the band gap, simply by changing the sign of  $\eta_o$ , keeping  $\omega_B$  fixed. As the band gap is solely determined by the rotation rate  $\omega_B$  and not the odd viscosity, we obtain an unusual topological phase transition that proceeds without band inversion or band gap closure [71]. This also allows a violation of the bulk-boundary correspondence, which can break down in the continuum [71, 177–181].

## Box 4: $\mathcal{PT}$ symmetry, exceptional points, and non-Hermitian skin modes.

The linear response of active media is often described by non-Hermitian operators, for example the dynamical matrix of an active solid  $D \neq D^\dagger$  [85]. Such systems exhibit a generalized parity-time ( $\mathcal{PT}$ ) symmetry [160,201,202] if there exists an antiunitary operator  $X$  such that  $[X, D] = 0$ . Depending on the relative strength of gain and loss, two cases arise: (i) the eigenvalues are all real ( $\mathcal{PT}$ -unbroken) and (ii) the eigenvalues come in complex conjugate pairs ( $\mathcal{PT}$ -broken). A familiar (passive) example is the damped harmonic oscillator (a):

$$\begin{bmatrix} \dot{p} \\ \dot{x} \end{bmatrix} = \begin{bmatrix} -\Gamma/M & -k \\ 1/M & 0 \end{bmatrix} \begin{bmatrix} p \\ x \end{bmatrix}$$

where  $M$  is the mass,  $\Gamma$  the damping coefficient and  $k$  the spring constant. Transitions between  $\mathcal{PT}$ -unbroken and  $\mathcal{PT}$ -broken states are generically accompanied by spectral singularities called exceptional points, where the two eigenvectors coalesce (red lines in b). For the harmonic oscillator, the exceptional point occurs at critical damping. An active example is given by solids whose bonds are described by the non-conservative force law  $\mathbf{F}(\mathbf{r}) = -(k\hat{\mathbf{r}} + k^a\hat{\phi})\delta r$  where  $\hat{\mathbf{r}}$  ( $\hat{\phi}$ ) is a unit vector pointing along (transverse to) the bond vector,  $\delta r$  is the change in length of the bond, and  $k$  and  $k^a$  are spring constants (c) [182]. When the bond is taken on a closed cycle, the work done  $W = \oint \mathbf{F} \cdot d\mathbf{r}$  is equal to  $k^a$  times the area enclosed by the path. The dynamical matrix that governs the motion of a single particle in the trap shown in (d) exhibits an exceptional point at a critical value of  $k_a/k = 1/\sqrt{3}$ .

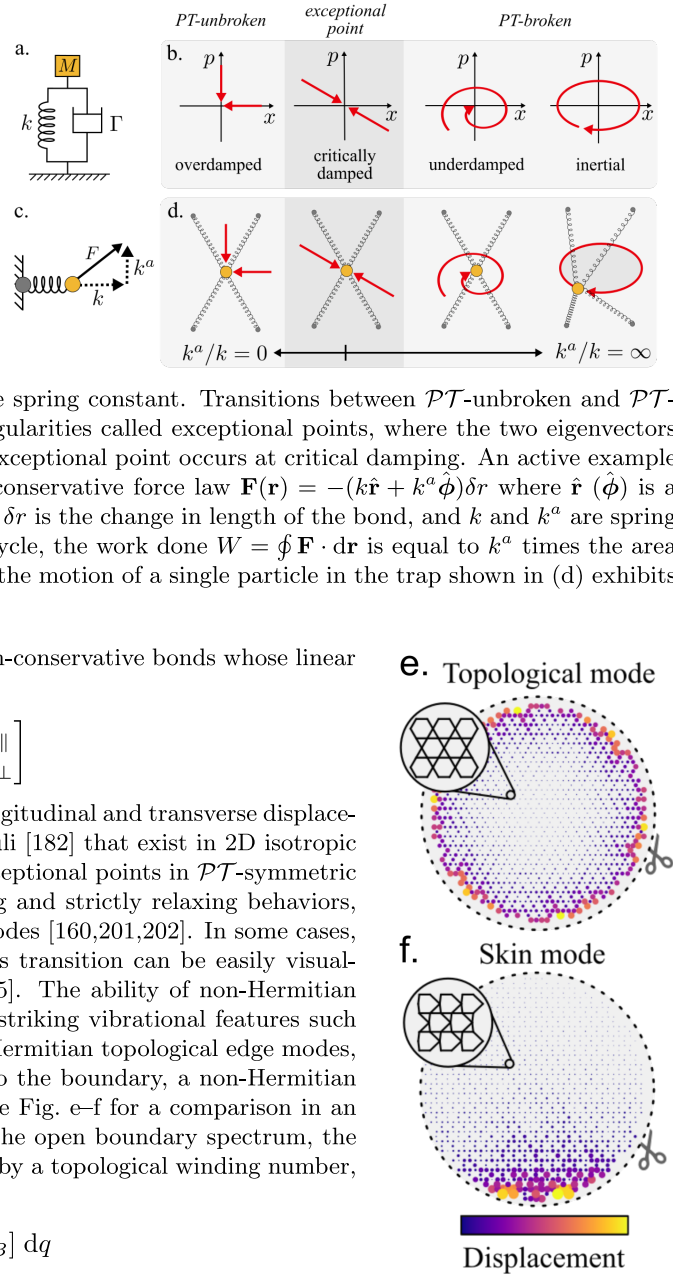
Similar phenomena occur in *overdamped* solids made of non-conservative bonds whose linear evolution can be expressed through a dynamical matrix

$$\Gamma \begin{bmatrix} \dot{u}_\parallel \\ \dot{u}_\perp \end{bmatrix} = q^2 \begin{bmatrix} B + \mu & K^o \\ -K^o - A & \mu \end{bmatrix} \begin{bmatrix} u_\parallel \\ u_\perp \end{bmatrix}$$

Here,  $u_\parallel(\mathbf{q})$  and  $u_\perp(\mathbf{q})$  indicate the Fourier modes of the longitudinal and transverse displacement field while  $K^o$  and  $A$  are two additional active moduli [182] that exist in 2D isotropic media along with the bulk and shear moduli  $B$  and  $\mu$ . Exceptional points in  $\mathcal{PT}$ -symmetric systems generically mark the crossover between oscillating and strictly relaxing behaviors, which is accompanied by structural changes of the eigenmodes [160,201,202]. In some cases, e.g., the active spring and simple harmonic oscillator, this transition can be easily visualized as a crossover between linear and circular motion [85]. The ability of non-Hermitian systems to host non-orthogonal eigenvectors gives rise to striking vibrational features such as the non-Hermitian skin effect [85,157,162,163]. Unlike Hermitian topological edge modes, in which a sub-extensive number of modes are localized to the boundary, a non-Hermitian system exhibits skin modes whose number is extensive, see Fig. e–f for a comparison in an active mechanical lattice [85]. For each eigenvalue  $\lambda_B$  in the open boundary spectrum, the localization of the corresponding eigenmode is determined by a topological winding number,  $\nu$  [161,187]:

$$\nu \equiv \frac{1}{2\pi i} \int_0^{2\pi} \frac{d}{dq} \ln[\lambda(q) - \lambda_B] dq$$

calculated from the eigenvalues  $\lambda(q)$  of the dynamical matrix under periodic boundary conditions. When  $\nu$  is nonzero, the corresponding eigenmode is localized either to the top or to the bottom depending on the sign of  $\nu$ . Note that this is only possible for complex eigenvalues. In Fig. 3b, for instance, the frequency of a skin mode in an active beam (star) is encircled by the periodic boundary spectrum (solid line). We emphasize that the non-Hermitian topological invariant  $\nu$  distinguishes inequivalent paths in the complex eigenvalue plane whereas the Chern number  $C$  measures the winding of the eigenstates (Box 3). Active and robotic metamaterials that exhibit non-Hermitian band topology and exceptional points are shown in Fig. 3.



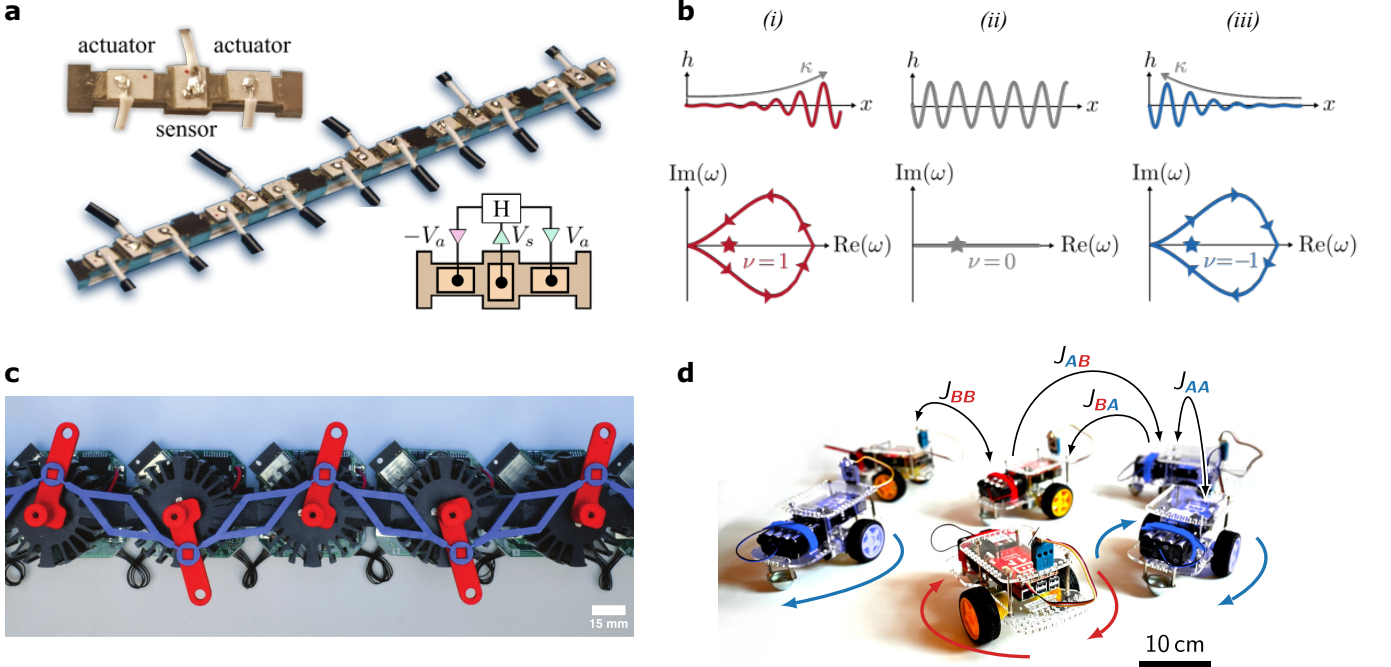


**FIG. 3. Topology and exceptional points in active and robotic metamaterials:** (a) Experimental realization of a self-sensing metabeam with active elasticity. A single unit cell featuring three piezoelectric patches: one that acts as a sensor, and two that act as actuators. Each unit cell has an electronic feedback. (b) Eigenmodes with open periodic boundary conditions with frequency corresponding to the star in the bottom panels. The localization of this eigenmode is determined by the sign of the winding of the energy in the complex plane. Sketches of the spectrum with periodic boundaries for each of the three cases: (i) right, (ii) no, and (iii) left localization. The arrows indicate directions of increasing wave number  $k$ . (a-b) are adapted from Ref. [161]. (c) A robotic metamaterial composed of an array of sensors and motors (black, with red rods attached) coupled together by soft elastic beams (blue). The motors enforce non-reciprocal interactions in response to forces exerted by neighbors and detected using the sensors. The edge of this one-dimensional metamaterial realizes modes corresponding to a non-Hermitian skin effect. Adapted from Ref. [162]. (d) A swarm of robots programmed to interact as non-reciprocal spins [62]. Instead of (anti)aligning like an (anti)ferromagnet, they spontaneously rotate either clockwise or counterclockwise, despite having no average natural frequency. The robotic spins are separated in two populations A (blue) and B (red). The intraspecies exchange interaction  $J_{AA}$  and  $J_{BB}$  are reciprocal, but the interspecies interactions are not, with  $J_{AB} \approx -J_{BA}$ . If self-propulsion is switched on, non-reciprocal flocking models exhibiting exceptional points are necessary to describe the behavior of the robotic swarm. A time-dependent phase with spontaneously broken chiral symmetry emerges in which self-propelled robots run in circles, either clockwise or counterclockwise, despite the absence of any external torque, adapted from Ref. [62].

#### D. Non-Hermitian skin effect in active media

In active matter, the combination of activity and dissipation naturally leads to the emergence of non-Hermitian operators. A growing number of theoretical [62, 71, 85, 182–184] and experimental [161, 163, 185] investigations examine the correspondence between the linear waves in active matter and the non-Hermitian topological band theory arising in open quantum systems [38, 158–160].

One of the more striking features of such systems is the emergence of the non-Hermitian skin effect [38, 83–85, 157, 158, 161, 183–186]. In solid elastic medium, a (generalized) restoring force  $\mathbf{F}(\mathbf{q}) = D(\mathbf{q})\mathbf{u}(\mathbf{q})$  occurs as a result of a displacement  $\mathbf{u}$  from equilibrium, such as the angular displacement of a robotic rotor [162, 185] or the shearing and bending of an active metabeam [161], in which  $D(\mathbf{q})$  is a dynamical matrix. The non-Hermitian

skin effect is a topological phenomenon unique to linear waves governed by a non-Hermitian dynamical matrix or Hamiltonian. The salient features of systems that exhibit the non-Hermitian skin effect are explained in detail in Box 4 and illustrated by concrete mechanical-metamaterial realizations in Fig. 3. Under periodic boundary conditions, these systems have a band structure that winds in the complex plane. When boundaries are introduced into the system, the spectrum dramatically changes its configuration in the complex plane. This spectral change is accompanied by an extensive number of vibrational states of the system which are localized at its edge. As explained in Box 4, the skin effect is characterized by a non-Hermitian winding number [83, 84, 187] distinct from the Chern number discussed in previous sections and Box 3.

Various strategies have been devised to produce and control the non-Hermitian skin effect in active mechanical

metamaterials (Fig. 3a-c), which mainly rely on breaking some notion of reciprocity [62, 188–194]. For example, Ref. [185] uses a 1D chain of coupled non-reciprocal robots whose motors effectively violate Newton’s third law (see Fig. 3c), similar to what has been observed in 1D microfluid crystals [195]. In this case, the presence of non-Hermitian skin modes can be rationalized using a simplified heuristic argument. Since the forces (or torques) at the two ends of a non-reciprocal bond are not equal and opposite, there is a net momentum flux across each bond. As a result, energy accumulates at one of the two ends of an open chain determined by the direction of the force imbalance.

By contrast, Refs. [85, 184] consider different classes of models in 1D and 2D in which Newton’s third law is still preserved, but the basic microscopic bonds violate Maxwell-Betti reciprocity that can be loosely defined as the symmetry between perturbation and response [161, 196]. In Ref. [161], piezoelectric components are used to build an active metabeam that conserves linear and angular momentum but is described by an elastic modulus that violates both parity and reciprocity (Fig. 3a–b). In all these systems, the skin effect can be observed and its existence inferred from either lattice models [183–185, 197] or from continuum equations based only on symmetries and conservation laws [85, 161].

Another type of topological objects unique to the spectrum of non-Hermitian systems are exceptional points and rings [198, 199], see Box 4 for precise mathematical definitions. Hermitian Hamiltonians and dynamical matrices can be diagonalized in a basis of orthogonal normal modes of vibration. In the presence of gain or loss, the eigenmodes can become non-orthogonal. Extreme cases can emerge in which two modes coalesce and the dynamical matrix becomes defective. Such points are known as exceptional points [198] and they can mediate topological phase transitions in non-Hermitian mechanical systems [85, 200]. Though active solids need not to have an Hermitian dynamical matrix, they often exhibit a property referred to as (generalized) parity-time ( $\mathcal{PT}$ ) symmetry [160, 201, 202], described in detail in Box 4. A crucial feature is that exceptional points occur at transitions between  $\mathcal{PT}$ -broken and  $\mathcal{PT}$ -unbroken phases, see top Figure in Box 4, which is often accompanied by pattern formation [62, 193, 194]. In certain cases, additional symmetries can ensure that the exceptional points form 1D manifolds in the Brillouin zone known as exceptional lines or rings [85, 203].

### III. OUTLOOK

Notions from topology and geometry offer a new perspective on active matter and provide unconventional tools for classifying the complex behavior of these far-from-equilibrium systems. Although abstract, topological techniques are becoming increasingly commonplace in the study of active systems. The success of topology,

just as in equilibrium materials, is rooted in the identification of robust collective degrees of freedom and excitations, which in active matter often acquire dramatic properties. The field is burgeoning and fast-paced, but it is still at a nascent stage, and this review only scratches the surface of topological active matter.

Exploring the relevance of topological properties of active systems to biology is perhaps one of the most ambitious avenues in the field. While defects in tissues have been noted as mechanically active centers of morphogenesis [99, 100, 144, 145], our understanding of the interplay between active forcing and tissue response in manipulating cell organization is still limited. Integrating biologically relevant mechanisms such as growth, cell differentiation, and mechanotransduction with the physics of active fluids would be crucial to this end. On a different scale, although biofilament-motor assemblies routinely display defects when reconstituted *in-vitro* [37, 88, 96], the relation of these phenomena to *in-vivo* cortical organization [150, 151, 204] remains mysterious and continues to be an open question. During development at the organ and organismal level, both collective motion and pattern formation are ubiquitous [205, 206], which offers an intriguing possibility for the realization of exotic topologically protected states. Recent studies have also suggested a role for topological states in nonequilibrium stochastic networks [207], in evolutionary population dynamics [208], and in the disassembly of biofilaments [20]. One challenge faced by future theoretical work is the robustness of topological states to biologically relevant perturbations. In this regard, more systematic experimental investigations are needed.

Active metamaterials and synthetic active matter offer a broad platform to engineer and apply novel topological states [30, 134]. Controlling and patterning defects using activity gradients has already emerged as an exciting direction of research [78, 136, 155]. While the main focus so far has been on two-dimensional systems, topological states in three dimensions offer new possibilities, including more complex defect textures [104] and topological degeneracies in band structure such as Weyl nodes [209, 210]. Designing synthetic gauge fields [68, 131, 211] and exceptional points in active fluids and solids [62, 85, 182] would be a powerful strategy to exploit these states for sensing and transport. Active flow is already being exploited, for example, to enhance *in-vitro* fertilization [212, 213], and creating topologically protected transport could be a route towards new technologies based on active matter.

From a theoretical perspective, important questions remain. Beyond topological band theory, the role of nonequilibrium noise and nonlinear interactions within active materials remains largely unexplored [62, 193, 194]. As discussed extensively, topological defects in active systems acquire much of their novelty from their dynamics [79]. Although much work has been done, a detailed understanding of defect-driven phase transitions and exotic defect-ordered states remain elusive. Towards

this end, comparing and contrasting active defects with the novel collective dynamics of vortices in open quantum systems and driven dissipative condensates [42, 43, 214] promises to be a fruitful endeavour.

## ACKNOWLEDGMENTS

The work of MJB was supported in part by the National Science Foundation under Grant No. NSF PHY-1748958 and NSF DMREF program, via Grant No. DMREF-1435794. MCM was primarily supported by the National Science Foundation under Grant No. DMR-1938187, with additional support from DMR-1720256 (iSuperSeed). SS is supported by the Harvard Society of Fellows. VV was supported by the Complex Dynamics and Systems Program of the Army Research Office under grant W911NF-19-1-0268, by the Simons Foundation and by the University of Chicago Materials Research

Science and Engineering Center, which is funded by the National Science Foundation under award number DMR-2011854. SS and AS gratefully acknowledge discussions during the 2019 summer workshop on “Active and Driven Matter: Connecting Quantum and Classical Systems” at the Aspen Center for Physics, which is supported by National Science Foundation grant PHY-1607611. The participation of AS at the Aspen Center for Physics was supported by the Simons Foundation. AS acknowledges the support of the Engineering and Physical Sciences Research Council (EPSRC) through New Investigator Award No. EP/T000961/1. We also acknowledge illuminating discussions throughout the virtual 2020 KITP program on “Symmetry, Thermodynamics and Topology in Active Matter”, which was supported in part by the National Science Foundation under Grant No. NSF PHY-1748958. We thank M. Fruchart, C. Scheibner, G. Baardink, and J. Binysh for inspiring conversations and suggestions.

- 
- [1] Berezinskii, V. Destruction of long-range order in one-dimensional and two-dimensional systems having a continuous symmetry group i. classical systems. *Soviet Journal of Experimental and Theoretical Physics* **32**, 493 (1971). [ZhETF 59, 907 (1971)].
  - [2] Berezinskii, V. Destruction of long-range order in one-dimensional and two-dimensional systems possessing a continuous symmetry group ii. quantum systems. *Soviet Journal of Experimental and Theoretical Physics* **34**, 610 (1972). [ZhETF 61, 1144 (1972)].
  - [3] Kosterlitz, J. M. & Thouless, D. J. Ordering, metastability and phase transitions in two-dimensional systems. *Journal of Physics C: Solid State Physics* **6**, 1181 (1973).
  - [4] Kosterlitz, J. The critical properties of the two-dimensional xy model. *Journal of Physics C: Solid State Physics* **7**, 1046 (1974).
  - [5] Mermin, N. D. The topological theory of defects in ordered media. *Reviews of Modern Physics* **51**, 591 (1979).
  - [6] Alexander, G. P., Chen, B. G.-g., Matsumoto, E. A. & Kamien, R. D. Colloquium: Disclination loops, point defects, and all that in nematic liquid crystals. *Reviews of Modern Physics* **84**, 497 (2012).
  - [7] Asorey, M. Space, matter and topology. *Nature Physics* **12**, 616 (2016).
  - [8] Wang, J. & Zhang, S.-C. Topological states of condensed matter. *Nature materials* **16**, 1062–1067 (2017).
  - [9] Kohmoto, M. Topological invariant and the quantization of the hall conductance. *Annals of Physics* **160**, 343–354 (1985).
  - [10] Moore, J. E. The birth of topological insulators. *Nature* **464**, 194 (2010).
  - [11] Chaikin, P. M. & Lubensky, T. C. *Principles of condensed matter physics* (Cambridge university press, 2000).
  - [12] Nelson, D. R. *Defects and geometry in condensed matter physics* (Cambridge University Press, 2002).
  - [13] Kosterlitz, J. M. Kosterlitz-thouless physics: a review of key issues. *Reports on Progress in Physics* **79**, 026001 (2016).
  - [14] Hasan, M. Z. & Kane, C. L. Colloquium: topological insulators. *Reviews of Modern Physics* **82**, 3045 (2010).
  - [15] Qi, X.-L. & Zhang, S.-C. Topological insulators and superconductors. *Reviews of Modern Physics* **83**, 1057 (2011).
  - [16] Fruchart, M. & Carpentier, D. An introduction to topological insulators. *Comptes Rendus Physique* **14**, 779 – 815 (2013).
  - [17] Asbóth, J. K., Oroszlány, L. & Pályi, A. *A Short Course on Topological Insulators* (Springer International Publishing, 2016).
  - [18] Halperin, B. I. Quantized hall conductance, current-carrying edge states, and the existence of extended states in a two-dimensional disordered potential. *Physical Review B* **25**, 2185 (1982).
  - [19] Aasen, D. et al. Milestones toward majorana-based quantum computing. *Physical Review X* **6**, 031016 (2016).
  - [20] Prodan, E. & Prodan, C. Topological phonon modes and their role in dynamic instability of microtubules. *Physical review letters* **103**, 248101 (2009).
  - [21] Huber, S. D. Topological mechanics. *Nature Physics* **12**, 621 (2016).
  - [22] Mao, X. & Lubensky, T. C. Maxwell lattices and topological mechanics. *Annual Review of Condensed Matter Physics* **9**, 413–433 (2018).
  - [23] Haldane, F. D. M. & Raghu, S. Possible realization of directional optical waveguides in photonic crystals with broken time-reversal symmetry. *Physical Review Letters* **100**, 013904 (2008).
  - [24] Ozawa, T. et al. Topological photonics. *Reviews of Modern Physics* **91**, 015006 (2019).
  - [25] Zhang, X., Xiao, M., Cheng, Y., Lu, M.-H. & Christensen, J. Topological sound. *Communications Physics* **1**, 1–13 (2018).
  - [26] Ramaswamy, S. The mechanics and statistics of active matter. *Annu. Rev. Condens. Matter Phys.* **1**, 323–345 (2010).

- [27] Marchetti, M. C. *et al.* Hydrodynamics of soft active matter. *Reviews of Modern Physics* **85**, 1143 (2013).
- [28] Ramaswamy, S. Active matter. *Journal of Statistical Mechanics: Theory and Experiment* **2017**, 054002 (2017).
- [29] Cavagna, A. & Giardina, I. Bird flocks as condensed matter. *Annu. Rev. Condens. Matter Phys.* **5**, 183–207 (2014).
- [30] Needleman, D. & Dogic, Z. Active matter at the interface between materials science and cell biology. *Nature Reviews Materials* **2**, 17048 (2017).
- [31] Trepaut, X. & Sahai, E. Mesoscale physical principles of collective cell organization. *Nature Physics* **14**, 671–682 (2018).
- [32] Palacci, J., Sacanna, S., Steinberg, A. P., Pine, D. J. & Chaikin, P. M. Living crystals of light-activated colloidal surfers. *Science* **339**, 936–940 (2013).
- [33] Bricard, A., Caussin, J.-B., Desreumaux, N., Dauchot, O. & Bartolo, D. Emergence of macroscopic directed motion in populations of motile colloids. *Nature* **503**, 95 (2013).
- [34] Narayan, V., Ramaswamy, S. & Menon, N. Long-lived giant number fluctuations in a swarming granular nematic. *Science* **317**, 105–108 (2007). Also see Supporting Information, page 4.
- [35] Rubenstein, M., Cornejo, A. & Nagpal, R. Programmable self-assembly in a thousand-robot swarm. *Science* **345**, 795–799 (2014).
- [36] Schaller, V., Weber, C., Semmrich, C., Frey, E. & Bausch, A. R. Polar patterns of driven filaments. *Nature* **467**, 73–77 (2010).
- [37] Sanchez, T., Chen, D. T., DeCamp, S. J., Heymann, M. & Dogic, Z. Spontaneous motion in hierarchically assembled active matter. *Nature* **491**, 431–434 (2012).
- [38] Ashida, Y., Gong, Z. & Ueda, M. Non-hermitian physics (2020). 2006.01837.
- [39] Bergholtz, E. J., Budich, J. C. & Kunst, F. K. Exceptional topology of non-hermitian systems (2019). 1912.10048.
- [40] Ota, Y. *et al.* Active topological photonics. *Nanophotonics* **9**, 547–567 (2020).
- [41] Sieberer, L., Huber, S. D., Altman, E. & Diehl, S. Dynamical critical phenomena in driven-dissipative systems. *Physical review letters* **110**, 195301 (2013).
- [42] Altman, E., Sieberer, L. M., Chen, L., Diehl, S. & Toner, J. Two-dimensional superfluidity of exciton polaritons requires strong anisotropy. *Physical Review X* **5**, 011017 (2015).
- [43] Alicea, J., Balents, L., Fisher, M. P., Paramekanti, A. & Radzihovsky, L. Transition to zero resistance in a two-dimensional electron gas driven with microwaves. *Physical Review B* **71**, 235322 (2005).
- [44] Hanai, R., Edelman, A., Ohashi, Y. & Littlewood, P. B. Non-hermitian phase transition from a polariton bose-einstein condensate to a photon laser. *Physical Review Letters* **122**, 185301 (2019).
- [45] Hanai, R. & Littlewood, P. B. Critical fluctuations at a many-body exceptional point. *Physical Review Research* **2**, 033018 (2020).
- [46] Gnesotto, F., Mura, F., Gladrow, J. & Broedersz, C. P. Broken detailed balance and non-equilibrium dynamics in living systems: a review. *Reports on Progress in Physics* **81**, 066601 (2018).
- [47] Seifert, U. From stochastic thermodynamics to thermodynamic inference. *Annual Review of Condensed Matter Physics* **10**, 171–192 (2019).
- [48] Forster, D. *Hydrodynamic fluctuations, broken symmetry, and correlation functions* (CRC Press, 2018).
- [49] Colen, J. *et al.* Machine learning active-nematic hydrodynamics (2020). 2006.13203.
- [50] Lu, P. Y., Kim, S. & Soljačić, M. Extracting interpretable physical parameters from spatiotemporal systems using unsupervised learning. *Physical Review X* **10**, 031056 (2020).
- [51] Cichos, F., Gustavsson, K., Mehlig, B. & Volpe, G. Machine learning for active matter. *Nature Machine Intelligence* **2**, 94–103 (2020).
- [52] Hohenberg, P. C. & Halperin, B. I. Theory of dynamic critical phenomena. *Reviews of Modern Physics* **49**, 435 (1977).
- [53] Cross, M. C. & Hohenberg, P. C. Pattern formation outside of equilibrium. *Reviews of modern physics* **65**, 851 (1993).
- [54] Lamb, H. *Hydrodynamics* (University Press, 1924).
- [55] Toner, J. & Tu, Y. Long-range order in a two-dimensional dynamical xy model: how birds fly together. *Physical Review Letters* **75**, 4326 (1995).
- [56] Toner, J., Tu, Y. & Ramaswamy, S. Hydrodynamics and phases of flocks. *Annals of Physics* **318**, 170–244 (2005).
- [57] Ramaswamy, S., Simha, R. A. & Toner, J. Active nematics on a substrate: Giant number fluctuations and long-time tails. *EPL (Europhysics Letters)* **62**, 196 (2003).
- [58] Simha, R. A. & Ramaswamy, S. Hydrodynamic fluctuations and instabilities in ordered suspensions of self-propelled particles. *Physical review letters* **89**, 058101 (2002).
- [59] Voituriez, R., Joanny, J.-F. & Prost, J. Spontaneous flow transition in active polar gels. *EPL (Europhysics Letters)* **70**, 404 (2005).
- [60] Cates, M. E. & Tailleur, J. Motility-induced phase separation. *Annu. Rev. Condens. Matter Phys.* **6**, 219–244 (2015).
- [61] Marchetti, M. C., Fily, Y., Henkes, S., Patch, A. & Yllanes, D. Minimal model of active colloids highlights the role of mechanical interactions in controlling the emergent behavior of active matter. *Current Opinion in Colloid & Interface Science* **21**, 34–43 (2016).
- [62] Fruchart, M., Hanai, R., Littlewood, P. B. & Vitelli, V. Phase transitions in non-reciprocal active systems. *arXiv preprint arXiv:2003.13176* (2020).
- [63] Juelicher, F., Kruse, K., Prost, J. & Joanny, J.-F. Active behavior of the cytoskeleton. *Physics reports* **449**, 3–28 (2007).
- [64] Prost, J., Jülicher, F. & Joanny, J.-F. Active gel physics. *Nature Physics* **11**, 111 (2015).
- [65] Banerjee, S. & Marchetti, M. C. Continuum models of collective cell migration. In *Cell Migrations: Causes and Functions*, 45–66 (Springer, 2019).
- [66] Cates, M. E. Active field theories. *arXiv preprint arXiv:1904.01330* (2019).
- [67] Giomi, L., Bowick, M. J., Ma, X. & Marchetti, M. C. Defect annihilation and proliferation in active nematics. *Physical review letters* **110**, 228101 (2013).
- [68] Souslov, A., van Zuiden, B. C., Bartolo, D. & Vitelli, V. Topological sound in active-liquid metamaterials.

- Nature Physics* **13**, 1091 (2017).
- [69] Delplace, P., Marston, J. & Venaille, A. Topological origin of equatorial waves. *Science* **358**, 1075–1077 (2017).
- [70] Shankar, S., Bowick, M. J. & Marchetti, M. C. Topological sound and flocking on curved surfaces. *Physical Review X* **7**, 031039 (2017).
- [71] Souslov, A., Dasbiswas, K., Fruchart, M., Vaikuntanathan, S. & Vitelli, V. Topological waves in fluids with odd viscosity. *Physical review letters* **122**, 128001 (2019).
- [72] Tsai, J.-C., Ye, F., Rodriguez, J., Gollub, J. P. & Lubensky, T. C. A chiral granular gas. *Physical Review Letters* **94**, 214301 (2005).
- [73] Fürthauer, S., Stremmel, M., Grill, S. W. & Jülicher, F. Active chiral fluids. *The European physical journal E* **35**, 1–13 (2012).
- [74] Banerjee, D., Souslov, A., Abanov, A. G. & Vitelli, V. Odd viscosity in chiral active fluids. *Nature communications* **8**, 1–12 (2017).
- [75] Maitra, A. & Lenz, M. Spontaneous rotation can stabilise ordered chiral active fluids. *Nature communications* **10**, 1–6 (2019).
- [76] Soni, V. *et al.* The odd free surface flows of a colloidal chiral fluid. *Nature Physics* **15**, 1188–1194 (2019).
- [77] Shankar, S., Ramaswamy, S., Marchetti, M. C. & Bowick, M. J. Defect unbinding in active nematics. *Phys. Rev. Lett.* **121**, 108002 (2018).
- [78] Shankar, S. & Marchetti, M. C. Hydrodynamics of active defects: from order to chaos to defect ordering. *Physical Review X* **9**, 041047 (2019).
- [79] Doostmohammadi, A., Ignés-Mullol, J., Yeomans, J. M. & Sagués, F. Active nematics. *Nature communications* **9**, 3246 (2018).
- [80] Kumar, N., Soni, H., Ramaswamy, S. & Sood, A. Flocking at a distance in active granular matter. *Nature communications* **5**, 1–9 (2014).
- [81] Han, M. *et al.* Statistical mechanics of a chiral active fluid. *arXiv preprint arXiv:2002.07679* (2020).
- [82] Berdyugin, A. *et al.* Measuring hall viscosity of graphene's electron fluid. *Science* **364**, 162–165 (2019).
- [83] Zhang, K., Yang, Z. & Fang, C. Correspondence between winding numbers and skin modes in non-hermitian systems. *Phys. Rev. Lett.* **125**, 126402 (2020).
- [84] Okuma, N., Kawabata, K., Shiozaki, K. & Sato, M. Topological origin of non-hermitian skin effects. *Phys. Rev. Lett.* **124**, 086801 (2020).
- [85] Scheibner, C., Irvine, W. & Vitelli, V. Non-hermitian band topology in active and dissipative mechanical metamaterials. *arXiv preprint arXiv:2001.04969* (2020).
- [86] Vicsek, T., Czirók, A., Ben-Jacob, E., Cohen, I. & Shochet, O. Novel type of phase transition in a system of self-driven particles. *Physical Review Letters* **75**, 1226–1229 (1995).
- [87] Toner, J. & Tu, Y. Flocks, herds, and schools: A quantitative theory of flocking. *Physical review E* **58**, 4828 (1998).
- [88] Nédélec, F., Surrey, T., Maggs, A. C. & Leibler, S. Self-organization of microtubules and motors. *Nature* **389**, 305 (1997).
- [89] Surrey, T., Nédélec, F., Leibler, S. & Karsenti, E. Physical properties determining self-organization of motors and microtubules. *Science* **292**, 1167–1171 (2001).
- [90] Sumino, Y. *et al.* Large-scale vortex lattice emerging from collectively moving microtubules. *Nature* **483**, 448–452 (2012).
- [91] Schaller, V. & Bausch, A. R. Topological defects and density fluctuations in collectively moving systems. *Proceedings of the National Academy of Sciences* **110**, 4488–4493 (2013).
- [92] Köster, D. V. *et al.* Actomyosin dynamics drive local membrane component organization in an in vitro active composite layer. *Proceedings of the National Academy of Sciences* **113**, E1645–E1654 (2016).
- [93] Bricard, A. *et al.* Emergent vortices in populations of colloidal rollers. *Nature communications* **6**, 1–8 (2015).
- [94] Keber, F. C. *et al.* Topology and dynamics of active nematic vesicles. *Science* **345**, 1135–1139 (2014).
- [95] Ellis, P. W. *et al.* Curvature-induced defect unbinding and dynamics in active nematic toroids. *Nature Physics* **14**, 85 (2018).
- [96] Kumar, N., Zhang, R., de Pablo, J. J. & Gardel, M. L. Tunable structure and dynamics of active liquid crystals. *Science Advances* **4**, eaat7779 (2018).
- [97] Duclos, G., Erlenkämper, C., Joanny, J.-F. & Silberzan, P. Topological defects in confined populations of spindle-shaped cells. *Nature Physics* **13**, 58 (2017).
- [98] Blanch-Mercader, C. *et al.* Turbulent dynamics of epithelial cell cultures. *Physical review letters* **120**, 208101 (2018).
- [99] Saw, T. B. *et al.* Topological defects in epithelia govern cell death and extrusion. *Nature* **544**, 212 (2017).
- [100] Kawaguchi, K., Kageyama, R. & Sano, M. Topological defects control collective dynamics in neural progenitor cell cultures. *Nature* **545**, 327 (2017).
- [101] Hoffmann, L. A., Schakenraad, K., Merks, R. M. & Giomi, L. Chiral stresses in nematic cell monolayers. *Soft Matter* (2020).
- [102] Kruse, K., Joanny, J.-F., Jülicher, F., Prost, J. & Sekimoto, K. Aster, vortices, and rotating spirals in active gels of polar filaments. *Physical review letters* **92**, 078101 (2004).
- [103] Čopar, S., Aplinc, J., Kos, Ž., Žumer, S. & Ravnik, M. Topology of three-dimensional active nematic turbulence confined to droplets. *Physical Review X* **9**, 031051 (2019).
- [104] Duclos, G. *et al.* Topological structure and dynamics of three-dimensional active nematics. *Science* **367**, 1120–1124 (2020).
- [105] Binysh, J., Kos, Ž., Čopar, S., Ravnik, M. & Alexander, G. P. Three-dimensional active defect loops. *Physical Review Letters* **124**, 088001 (2020).
- [106] Whitfield, C. A. *et al.* Hydrodynamic instabilities in active cholesteric liquid crystals. *The European Physical Journal E* **40**, 50 (2017).
- [107] Metselaar, L., Doostmohammadi, A. & Yeomans, J. M. Topological states in chiral active matter: Dynamic blue phases and active half-skyrmions. *The Journal of chemical physics* **150**, 064909 (2019).
- [108] Thampi, S. P., Golestanian, R. & Yeomans, J. M. Velocity correlations in an active nematic. *Physical review letters* **111**, 118101 (2013).
- [109] Pismen, L. Dynamics of defects in an active nematic layer. *Physical Review E* **88**, 050502 (2013).
- [110] Giomi, L. Geometry and topology of turbulence in active nematics. *Physical Review X* **5**, 031003 (2015).

- [111] Wensink, H. H. *et al.* Meso-scale turbulence in living fluids. *Proceedings of the National Academy of Sciences* **109**, 14308–14313 (2012).
- [112] Hemingway, E. J., Mishra, P., Marchetti, M. C. & Fielding, S. M. Correlation lengths in hydrodynamic models of active nematics. *Soft Matter* **12**, 7943–7952 (2016).
- [113] Guillamat, P., Ignés-Mullol, J. & Sagués, F. Taming active turbulence with patterned soft interfaces. *Nature communications* **8**, 564 (2017).
- [114] Lemma, L. M., DeCamp, S. J., You, Z., Giomi, L. & Dogic, Z. Statistical properties of autonomous flows in 2d active nematics. *Soft matter* **15**, 3264–3272 (2019).
- [115] Khoromskaia, D. & Alexander, G. P. Vortex formation and dynamics of defects in active nematic shells. *New Journal of Physics* **19**, 103043 (2017).
- [116] Cortese, D., Eggers, J. & Liverpool, T. B. Pair creation, motion, and annihilation of topological defects in two-dimensional nematic liquid crystals. *Physical Review E* **97**, 022704 (2018).
- [117] Tang, X. & Selinger, J. V. Theory of defect motion in 2d passive and active nematic liquid crystals. *Soft Matter* **15**, 587–601 (2019).
- [118] Zhang, Y.-H., Deserno, M. & Tu, Z.-C. The dynamics of active nematic defects on the surface of a sphere. *arXiv preprint arXiv:2006.02947* (2020).
- [119] Vafa, F., Bowick, M. J., Marchetti, M. C. & Shraiman, B. I. Multi-defect dynamics in active nematics. *arXiv preprint arXiv:2007.02947* (2020).
- [120] Maitra, A., Lenz, M. & Voituriez, R. Chiral active hexatic: Giant number fluctuations, waves and destruction of order. *arXiv preprint arXiv:2004.09115* (2020).
- [121] Ambegaokar, V., Halperin, B., Nelson, D. R. & Siggia, E. D. Dynamics of superfluid films. *Physical Review B* **21**, 1806 (1980).
- [122] Zippelius, A., Halperin, B. & Nelson, D. R. Dynamics of two-dimensional melting. *Physical Review B* **22**, 2514 (1980).
- [123] DeCamp, S. J., Redner, G. S., Baskaran, A., Hagan, M. F. & Dogic, Z. Orientational order of motile defects in active nematics. *Nature materials* **14**, 1110–1115 (2015).
- [124] Putzig, E., Redner, G. S., Baskaran, A. & Baskaran, A. Instabilities, defects, and defect ordering in an over-damped active nematic. *Soft matter* **12**, 3854–3859 (2016).
- [125] Srivastava, P., Mishra, P. & Marchetti, M. C. Negative stiffness and modulated states in active nematics. *Soft Matter* **12**, 8214–8225 (2016).
- [126] Patelli, A., Djafer-Cherif, I., Aranson, I. S., Bertin, E. & Chaté, H. Understanding dense active nematics from microscopic models. *Physical Review Letters* **123**, 258001 (2019).
- [127] Doostmohammadi, A., Adamer, M. F., Thampli, S. P. & Yeomans, J. M. Stabilization of active matter by flow-vortex lattices and defect ordering. *Nature communications* **7**, 1–9 (2016).
- [128] Oza, A. U. & Dunkel, J. Antipolar ordering of topological defects in active liquid crystals. *New Journal of Physics* **18**, 093006 (2016).
- [129] Pearce, D. *et al.* Scale-free defect ordering in passive and active nematics. *arXiv preprint arXiv:2004.13704* (2020).
- [130] Thijssen, K., Nejad, M. R. & Yeomans, J. M. Large scale ordering of active defects. *arXiv preprint arXiv:2005.01164* (2020).
- [131] Chardac, A., Shankar, S., Marchetti, M. C. & Bartolo, D. Emergence of dynamic vortex glasses in disordered polar active fluids. *arXiv preprint arXiv:2002.12893* (2020).
- [132] Bechinger, C. *et al.* Active particles in complex and crowded environments. *Reviews of Modern Physics* **88**, 045006 (2016).
- [133] Opathalage, A. *et al.* Self-organized dynamics and the transition to turbulence of confined active nematics. *Proceedings of the National Academy of Sciences* **116**, 4788–4797 (2019).
- [134] Peng, C., Turiv, T., Guo, Y., Wei, Q.-H. & Lavrentovich, O. D. Command of active matter by topological defects and patterns. *Science* **354**, 882–885 (2016).
- [135] Turiv, T. *et al.* Topology control of human fibroblast cells monolayer by liquid crystal elastomer. *Science Advances* **6**, eaaz6485 (2020).
- [136] Ross, T. D. *et al.* Controlling organization and forces in active matter through optically defined boundaries. *Nature* **572**, 224–229 (2019).
- [137] Guillamat, P., Ignés-Mullol, J., Shankar, S., Marchetti, M. C. & Sagués, F. Probing the shear viscosity of an active nematic film. *Physical Review E* **94**, 060602 (2016).
- [138] Guillamat, P., Ignés-Mullol, J. & Sagués, F. Control of active liquid crystals with a magnetic field. *Proceedings of the National Academy of Sciences* **113**, 5498–5502 (2016).
- [139] Norton, M. M. *et al.* Insensitivity of active nematic liquid crystal dynamics to topological constraints. *Physical Review E* **97**, 012702 (2018).
- [140] Shendruk, T. N., Doostmohammadi, A., Thijssen, K. & Yeomans, J. M. Dancing disclinations in confined active nematics. *Soft Matter* **13**, 3853–3862 (2017).
- [141] Hardoüin, J. *et al.* Reconfigurable flows and defect landscape of confined active nematics. *Communications Physics* **2**, 1–9 (2019).
- [142] Sknepnek, R. & Henkes, S. Active swarms on a sphere. *Physical Review E* **91**, 022306 (2015).
- [143] Yaman, Y. I., Demir, E., Vetter, R. & Kocabas, A. Emergence of active nematics in chaining bacterial biofilms. *Nature communications* **10**, 1–9 (2019).
- [144] Copenhagen, K., Alert, R., Wingreen, N. S. & Shaevitz, J. W. Topological defects induce layer formation in myxococcus xanthus colonies. *arXiv preprint arXiv:2001.03804* (2020).
- [145] Maroudas-Sacks, Y. *et al.* Topological defects in the nematic order of actin fibers as organization centers of hydra morphogenesis. *bioRxiv preprint bioRxiv 2020.03.02.972539* (2020).
- [146] Guillamat, P., Blanch-Mercader, C., Kruse, K. & Roux, A. Integer topological defects organize stresses driving tissue morphogenesis. *bioRxiv* (2020).
- [147] Blanch-Mercader, C., Guillamat, P., Roux, A. & Kruse, K. Quantifying material properties of cell monolayers by analyzing integer topological defects. *arXiv preprint arXiv:2006.01575* (2020).
- [148] Doostmohammadi, A., Thampli, S. P. & Yeomans, J. M. Defect-mediated morphologies in growing cell colonies. *Physical review letters* **117**, 048102 (2016).
- [149] Metselaar, L., Yeomans, J. M. & Doostmohammadi, A. Topology and morphology of self-deforming active shells. *Physical Review Letters* **123**, 208001 (2019).

- [150] Brugués, J. & Needleman, D. Physical basis of spindle self-organization. *Proceedings of the National Academy of Sciences* **111**, 18496–18500 (2014).
- [151] Tan, T. H. *et al.* Topological turbulence in the membrane of a living cell. *Nature Physics* 1–6 (2020).
- [152] Genkin, M. M., Sokolov, A., Lavrentovich, O. D. & Aranson, I. S. Topological defects in a living nematic ensnare swimming bacteria. *Physical Review X* **7**, 011029 (2017).
- [153] Endresen, K. D., Kim, M. & Serra, F. Topological defects of integer charge in cell monolayers. *arXiv preprint arXiv:1912.03271* (2019).
- [154] Schuppler, M., Keber, F. C., Kröger, M. & Bausch, A. R. Boundaries steer the contraction of active gels. *Nature communications* **7**, 1–10 (2016).
- [155] Zhang, R. *et al.* Structuring stress for active materials control. *arXiv preprint arXiv:1912.01630* (2019).
- [156] Norton, M. M., Grover, P., Hagan, M. F. & Fraden, S. Optimal control of active nematics (2020). 2007.14837.
- [157] Yao, S. & Wang, Z. Edge states and topological invariants of non-hermitian systems. *Physical review letters* **121**, 086803 (2018).
- [158] Budich, J. C., Carlström, J., Kunst, F. K. & Bergholtz, E. J. Symmetry-protected nodal phases in non-hermitian systems. *Phys. Rev. B* **99**, 041406 (2019).
- [159] Hatano, N. & Nelson, D. R. Localization transitions in non-hermitian quantum mechanics. *Phys. Rev. Lett.* **77**, 570–573 (1996).
- [160] Bender, C. M. & Boettcher, S. Real spectra in non-hermitian hamiltonians having  $pt$  symmetry. *Phys. Rev. Lett.* **80**, 5243–5246 (1998).
- [161] Chen, Y., Li, X., Scheibner, C., Vitelli, V. & Huang, G. Self-sensing metamaterials with odd micropolarity. *arXiv preprint arxiv.2009.07329* (2020).
- [162] Brandenbourger, M., Locsin, X., Lerner, E. & Coulais, C. Non-reciprocal robotic metamaterials. *Nature communications* **10**, 1–8 (2019).
- [163] Yamauchi, L., Hayata, T., Uwamichi, M., Ozawa, T. & Kawaguchi, K. Chirality-driven edge flow and non-hermitian topology in active nematic cells (2020). arXiv:2008.10852.
- [164] Khanikaev, A. B., Fleury, R., Mousavi, S. H. & Alu, A. Topologically robust sound propagation in an angular-momentum-biased graphene-like resonator lattice. *Nature communications* **6**, 1–7 (2015).
- [165] Sone, K. & Ashida, Y. Anomalous topological active matter. *Physical Review Letters* **123**, 205502 (2019).
- [166] Carmo, M. P. d. *Riemannian geometry* (Birkhäuser, 1992).
- [167] Bertoldi, K., Vitelli, V., Christensen, J. & van Hecke, M. Flexible mechanical metamaterials. *Nature Reviews Materials* **2**, 1–11 (2017).
- [168] Yang, Z. *et al.* Topological acoustics. *Physical review letters* **114**, 114301 (2015).
- [169] Nash, L. M. *et al.* Topological mechanics of gyroscopic metamaterials. *Proceedings of the National Academy of Sciences* **112**, 14495–14500 (2015).
- [170] Wang, P., Lu, L. & Bertoldi, K. Topological phononic crystals with one-way elastic edge waves. *Physical Review Letters* **115**, 104302 (2015).
- [171] Mitchell, N. P., Nash, L. M., Hexner, D., Turner, A. M. & Irvine, W. T. M. Amorphous topological insulators constructed from random point sets. *Nature Physics* **14**, 380–385 (2018).
- [172] Fleury, R., Sounas, D. L., Sieck, C. F., Haberman, M. R. & Alù, A. Sound isolation and giant linear nonreciprocity in a compact acoustic circulator. *Science* **343**, 516–519 (2014).
- [173] Geyer, D., Morin, A. & Bartolo, D. Sounds and hydrodynamics of polar active fluids. *Nature materials* **17**, 789–793 (2018).
- [174] Cha, J., Kim, K. W. & Daraio, C. Experimental realization of on-chip topological nanoelectromechanical metamaterials. *Nature* **564**, 229–233 (2018).
- [175] Cummer, S. A., Christensen, J. & Alù, A. Controlling sound with acoustic metamaterials. *Nature Reviews Materials* **1**, 16001 (2016).
- [176] van Zuiden, B. C., Paulose, J., Irvine, W. T., Bartolo, D. & Vitelli, V. Spatiotemporal order and emergent edge currents in active spinner materials. *Proceedings of the national academy of sciences* **113**, 12919–12924 (2016).
- [177] Silveirinha, M. G. Proof of the bulk-edge correspondence through a link between topological photonics and fluctuation-electrodynamics. *Physical Review X* **9**, 011037 (2019).
- [178] Volovik, G. An analog of the quantum hall effect in a superfluid he-3 film. *Soviet Physics-JETP* **67**, 1804–1811 (1988).
- [179] Tauber, C., Delplace, P. & Venaille, A. Anomalous bulk-edge correspondence in continuous media. *Physical Review Research* **2**, 013147 (2020).
- [180] Bal, G. Continuous bulk and interface description of topological insulators. *Journal of Mathematical Physics* **60**, 081506 (2019).
- [181] Bal, G. Topological invariants for interface modes (2019). 1906.08345v2.
- [182] Scheibner, C. *et al.* Odd elasticity. *Nature Physics* 1–6 (2020).
- [183] Rosa, M. I. & Ruzzene, M. Dynamics and topology of non-hermitian elastic lattices with non-local feedback control interactions. *New Journal of Physics* **22**, 053004 (2020).
- [184] Zhou, D. & Zhang, J. Non-hermitian topological metamaterials with odd elasticity. *Phys. Rev. Research* **2**, 023173 (2020).
- [185] Ghatak, A., Brandenbourger, M., van Wezel, J. & Coulais, C. Observation of non-hermitian topology and its bulk-edge correspondence (2019). arXiv:1907.11619v1.
- [186] Lee, C. H. & Thomale, R. Anatomy of skin modes and topology in non-hermitian systems. *Phys. Rev. B* **99**, 201103 (2019).
- [187] Gong, Z. *et al.* Topological phases of non-hermitian systems. *Physical Review X* **8**, 031079 (2018).
- [188] Das, J., Rao, M. & Ramaswamy, S. Driven heisenberg magnets: Nonequilibrium criticality, spatiotemporal chaos and control. *Europhysics Letters (EPL)* **60**, 418–424 (2002).
- [189] Lahiri, R. & Ramaswamy, S. Are steadily moving crystals unstable? *Physical Review Letters* **79**, 1150–1153 (1997).
- [190] Uchida, N. & Golestanian, R. Synchronization and collective dynamics in a carpet of microfluidic rotors. *Physical Review Letters* **104**, 178103 (2010).
- [191] Saha, S., Ramaswamy, S. & Golestanian, R. Pairing, waltzing and scattering of chemotactic active colloids. *New Journal of Physics* **21**, 063006 (2019).

- [192] Gupta, R. K., Kant, R., Soni, H., Sood, A. K. & Ramaswamy, S. Active nonreciprocal attraction between motile particles in an elastic medium (2020). arXiv:2007.04860.
- [193] You, Z., Baskaran, A. & Marchetti, M. C. Nonreciprocity as a generic route to traveling states. *Proceedings of the National Academy of Sciences* **117**, 19767–19772 (2020).
- [194] Saha, S., Agudo-Canalejo, J. & Golestanian, R. Scalar active mixtures: The non-reciprocal cahn-hilliard model. *arXiv preprint arXiv:2005.07101* (2020).
- [195] Beatus, T., Tlusty, T. & Bar-Ziv, R. Phonons in a one-dimensional microfluidic crystal. *Nature Physics* **2**, 743–748 (2006).
- [196] Nassar, H. *et al.* Nonreciprocity in acoustic and elastic materials. *Nature Reviews Materials* 1–19 (2020).
- [197] Gao, P., Willatzen, M. & Christensen, J. Anomalous topological edge states in non-hermitian piezophononic media (2020). arXiv:2009.10508.
- [198] Heiss, W. The physics of exceptional points. *Journal of Physics A: Mathematical and Theoretical* **45**, 444016 (2012).
- [199] Kawabata, K., Bessho, T. & Sato, M. Classification of exceptional points and non-hermitian topological semimetals. *Phys. Rev. Lett.* **123**, 066405 (2019).
- [200] Shen, H., Zhen, B. & Fu, L. Topological band theory for non-hermitian hamiltonians. *Physical review letters* **120**, 146402 (2018).
- [201] Mostafazadeh, A. Pseudo-hermiticity versus pt symmetry: The necessary condition for the reality of the spectrum of a non-hermitian hamiltonian. *Journal of Mathematical Physics* **43**, 205–214 (2002).
- [202] Mostafazadeh, A. Physics of spectral singularities. In *Trends in Mathematics*, 145–165 (Springer International Publishing, 2015).
- [203] Yoshida, T. & Hatsugai, Y. Exceptional rings protected by emergent symmetry for mechanical systems. *Phys. Rev. B* **100**, 054109 (2019).
- [204] Gowrishankar, K. *et al.* Active remodeling of cortical actin regulates spatiotemporal organization of cell surface molecules. *Cell* **149**, 1353–1367 (2012).
- [205] Lecuit, T. & Mahadevan, L. Morphogenesis one century after on growth and form (2017).
- [206] Howard, J., Grill, S. W. & Bois, J. S. Turing’s next steps: the mechanochemical basis of morphogenesis. *Nature Reviews Molecular Cell Biology* **12**, 392–398 (2011).
- [207] Murugan, A. & Vaikuntanathan, S. Topologically protected modes in non-equilibrium stochastic systems. *Nature communications* **8**, 1–6 (2017).
- [208] Knebel, J., Geiger, P. M. & Frey, E. Topological phase transition in coupled rock-paper-scissor cycles (2020). arXiv:2009.01780.
- [209] Armitage, N., Mele, E. & Vishwanath, A. Weyl and dirac semimetals in three-dimensional solids. *Reviews of Modern Physics* **90**, 015001 (2018).
- [210] Fruchart, M. *et al.* Soft self-assembly of weyl materials for light and sound. *Proceedings of the National Academy of Sciences* **115**, E3655–E3664 (2018).
- [211] Abbaszadeh, H., Souslov, A., Paulose, J., Schomerus, H. & Vitelli, V. Sonic landau levels and synthetic gauge fields in mechanical metamaterials. *Physical Review Letters* **119**, 195502 (2017).
- [212] Denissenko, P., Kantsler, V., Smith, D. J. & Kirkman-Brown, J. Human spermatozoa migration in microchannels reveals boundary-following navigation. *Proceedings of the National Academy of Sciences* **109**, 8007–8010 (2012).
- [213] Kantsler, V., Dunkel, J., Blayney, M. & Goldstein, R. E. Rheotaxis facilitates upstream navigation of mammalian sperm cells. *Elife* **3**, e02403 (2014).
- [214] Wachtel, G., Sieberer, L., Diehl, S. & Altman, E. Electrodynamic duality and vortex unbinding in driven-dissipative condensates. *Physical Review B* **94**, 104520 (2016).